AGN BASICS: RADIATIVE MECHANISM

The radiative mechanism which fuels AGNs needs to explain:

- **Broad range of luminosities up to $L \sim 10^{13} L_{\odot}$**
- **Collimated relativistic jets of particles of sizes up to Mpc scale**
- **Stable gyroscope on timescale of 10^7 yr**
- **Energy up to $\Delta E \sim 10^{61}$ erg**
  - **Assuming $\Delta E = \varepsilon Mc^2$, implies $\varepsilon \sim 10\%$, a very large energy production efficiency (e.g. for nuclear reaction ε is of the order of a few percent)**
- **Strong and broad optical/UV emission lines**
- **Emission over a very broad band**
- **Variability**

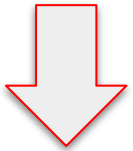

Black Hole + Accretion Disk Model

BLACK HOLE + ACCRETION DISK MODEL

Eddington limit:

- **Accretion of material on the disk produces radiation → radiation makes pressure which inhibit further accretion**
- **The Eddington limit corresponds to the luminosity at which the radiation drag equals the gravitational force**

$$F_{rad} = \frac{L\sigma_T}{4\pi c r^2} = F_{grav} = \frac{GM(m_p + m_e)}{r^2} \quad \rightarrow L \leq L_{Edd} = \frac{4\pi GMm_p c}{\sigma_T}$$

$$(m_p >> m_e)$$

Note: Radiation pressure acts on electrons; but electrons and ions (protons) cannot separate because of Coulomb force

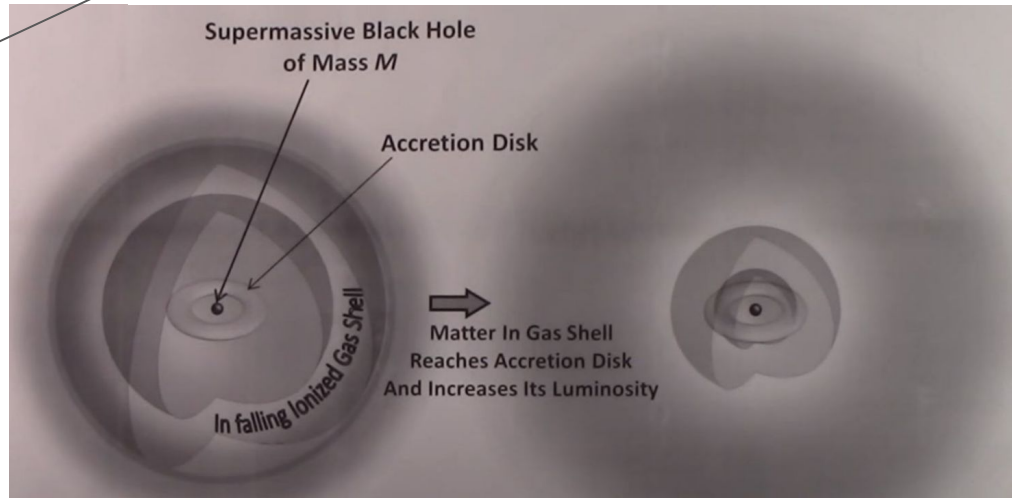

BLACK HOLE + ACCRETION DISK MODEL

Sagittarius - A :

- **Dynamical mass of Sagittarius – A**

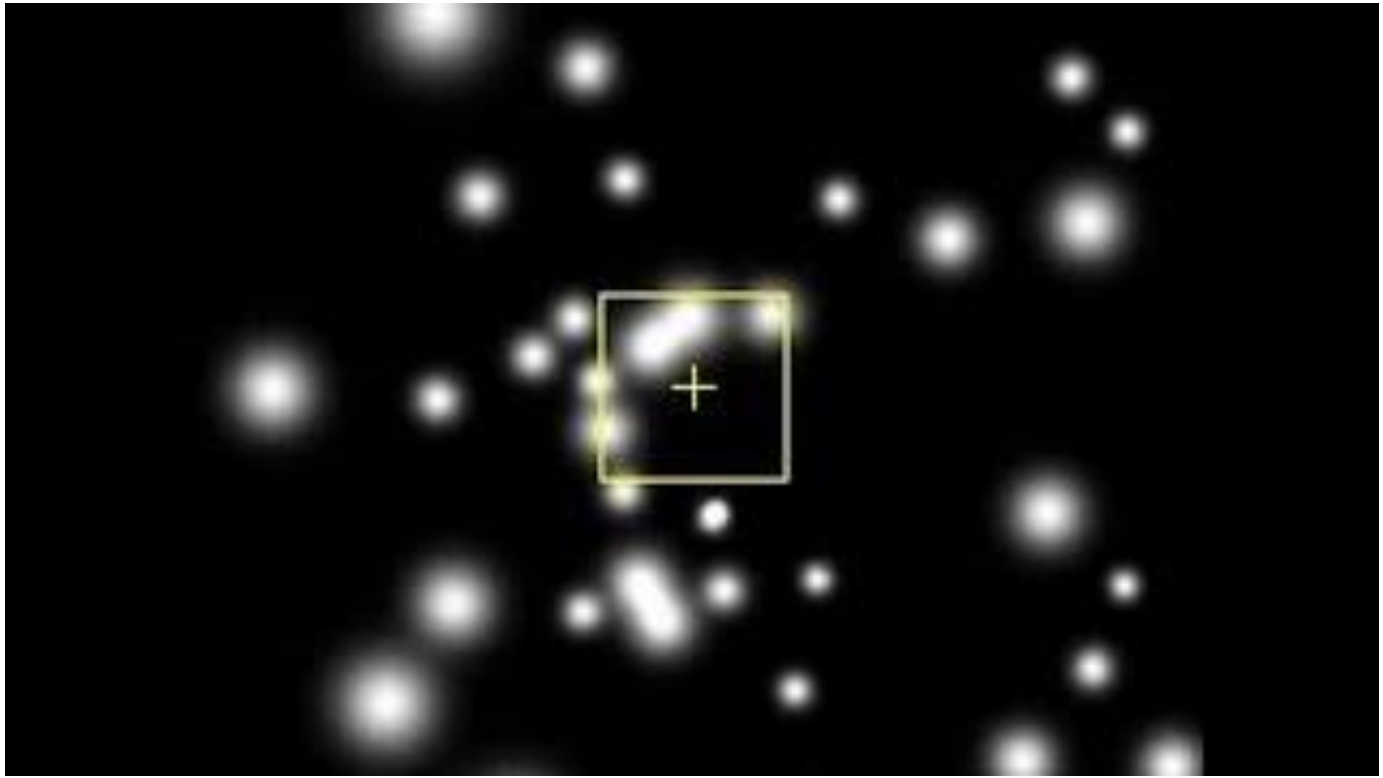

BLACK HOLE + ACCRETION DISK MODEL

Sgt A*: S2 star dynamical mass

Fitting orbit and radial velocities:
Period ~15.8 y
Eccentricity ~ 0.87
Semi-major axis ~1025 AU
Pericenter ~ 125 AU

Using Kepler's third law:

$$\left(\frac{2\pi}{P}\right)^2 = \frac{GM}{a^3}$$

$$M = \mathrm{M}_\odot \left(\frac{a}{1\,\mathrm{AU}}\right)^3 \left(\frac{P}{1\,\mathrm{yr}}\right)^{-2}$$

$$M = 4.3 \times 10^6\,\mathrm{M}_\odot \left(\frac{a}{1025\,\mathrm{AU}}\right)^3 \left(\frac{P}{15.8\,\mathrm{yr}}\right)^{-2}$$

→ few 10^6 $M_\odot$ within ~10s AU → Massive Black Hole

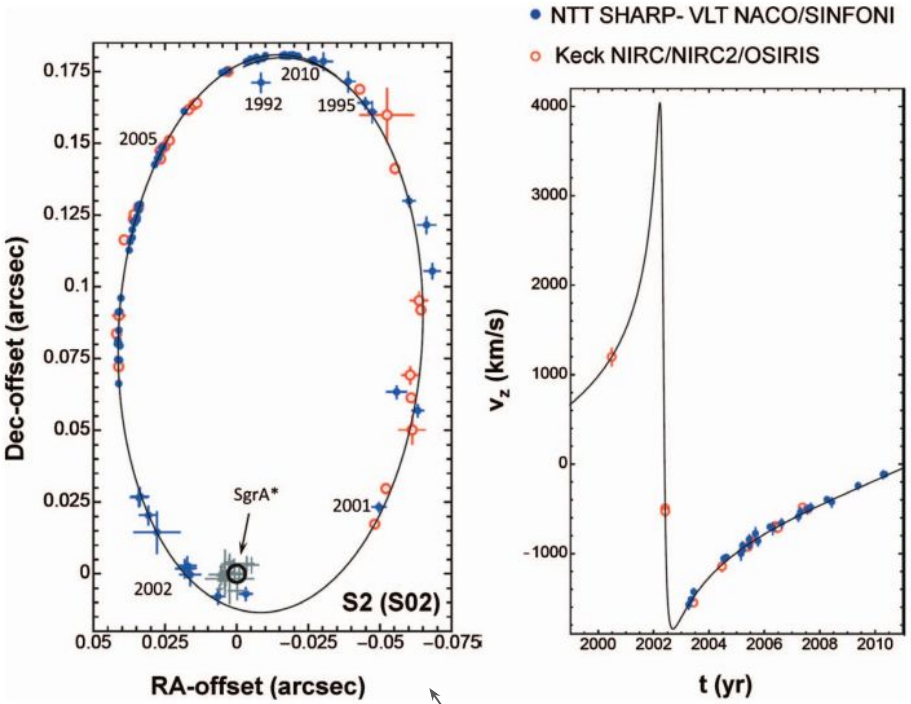

Orbit is not closed for possible proper motion of the BH
Grey crosses are IR flares

BLACK HOLE + ACCRETION DISK MODEL

Other methods to estimate the BH masses:

TABLE I

Probing the centers of galaxies.

Method & Telescope	Scale (R_S)	No. of SBH Detections	$M_\bullet$ Range ($M_\odot$)	Typical Densities ($M_\odot$ pc^{-3})
Fe Kα line (XEUS, ConX)	3–10	0	N/A	N/A
Reverberation mapping (Ground based optical)	600	36	10^6–4×10^8	$\gtrsim 10^{10}$
Stellar proper motion (Keck, NTT, VLT)	1000	1	4×10^6	4×10^{16}
H_2O megamasers (VLBI)	10^4	1	4×10^7	4×10^9
Gas dynamics (optical) (Mostly *HST*)	10^6	11	7×10^7–4×10^9	$\sim 10^5$
Stellar dynamics (Mostly *HST*)	10^6	17	10^7–3×10^9	$\sim 10^5$

The columns give all methods which can (or, in the case of the Fe Kα line emission, might) be used

Ferrarese & Ford 2005

BLACK HOLE + ACCRETION DISK MODEL

AGN Spectral Energy Distribution:

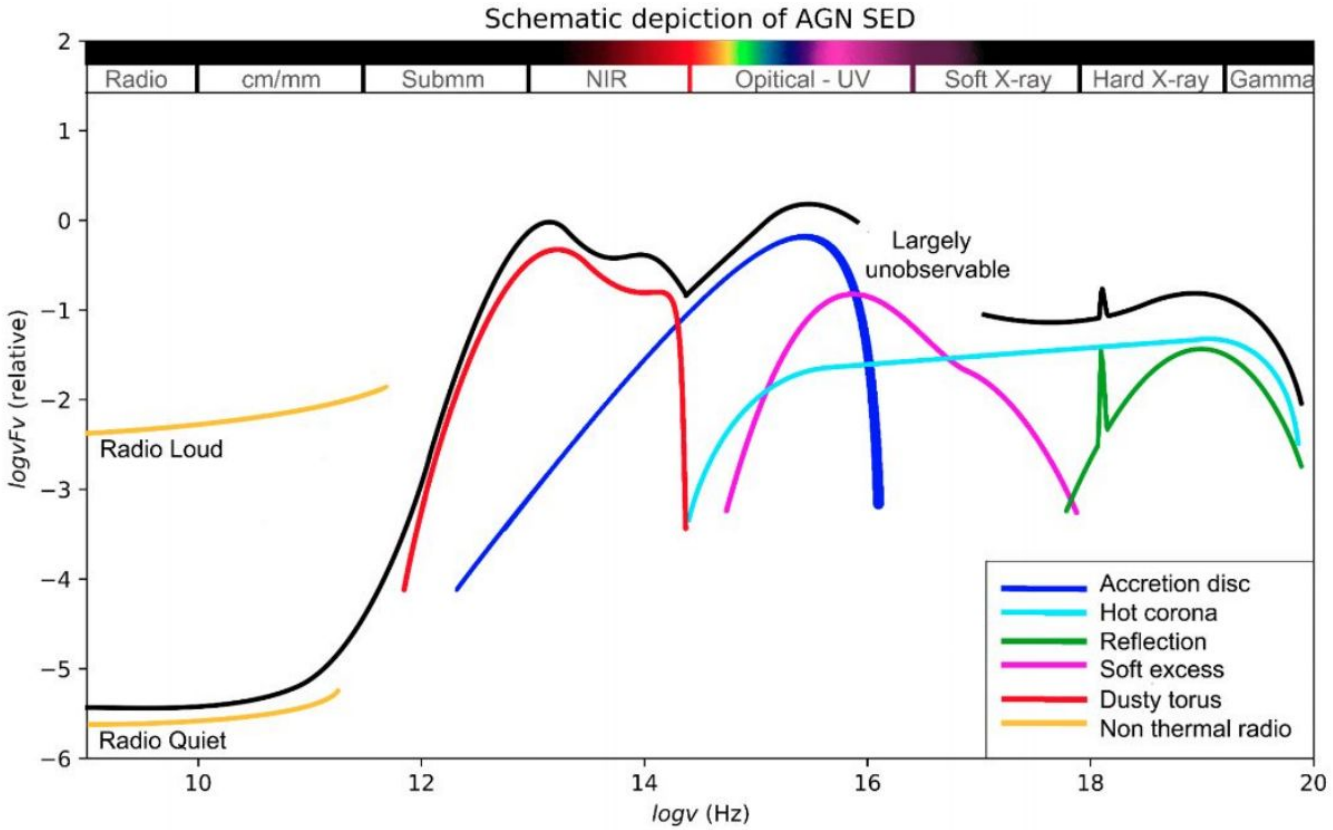

BLACK HOLE + ACCRETION DISK MODEL

Origin of the X-ray emission:

- **X-rays are not naturally produced by AGN disks; the disk is too cool**
- **Need to add an accretion disk "corona" with a temperature of ~ 150 keV → this makes X-rays by Compton scattering**
- **Perhaps low-energy X-ray from disk component (soft X-ray excess)**

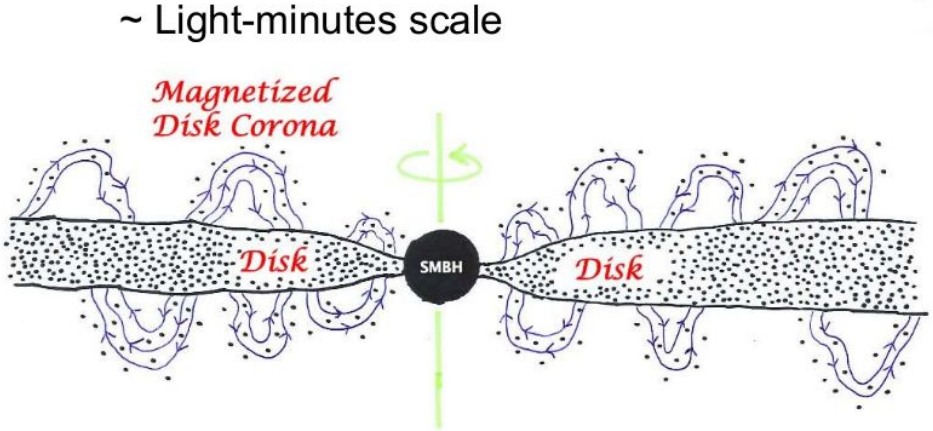

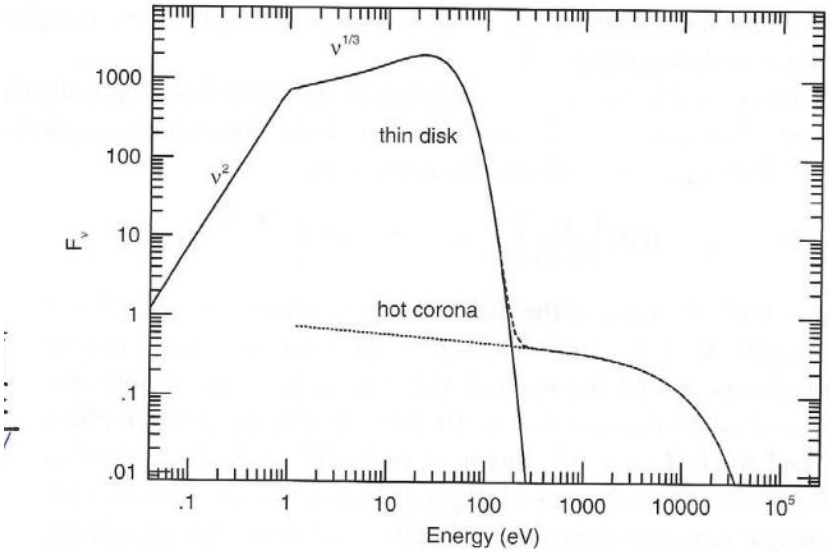

ure 4.3. A schematic of a combined disk–corona spectrum. The maximum temperature of the geometrically thin, optically thick accretion disk is $T_{max} = 10^5$ K, and its outer boundary temperature is determined by the conditions at the self-gravity radius. The disk is surrounded by an optically thin corona with $T_{cor} = 10^8$ K.

BLACK HOLE + ACCRETION DISK MODEL

Obscuration and radiation reprocessing:

- **Many active galaxies have obscuring / reprocessing material, often envisioned to be in the form of a “torus”**
- **This material likely produces much of the infrared emission as reprocessed “waste heat” from dust.**

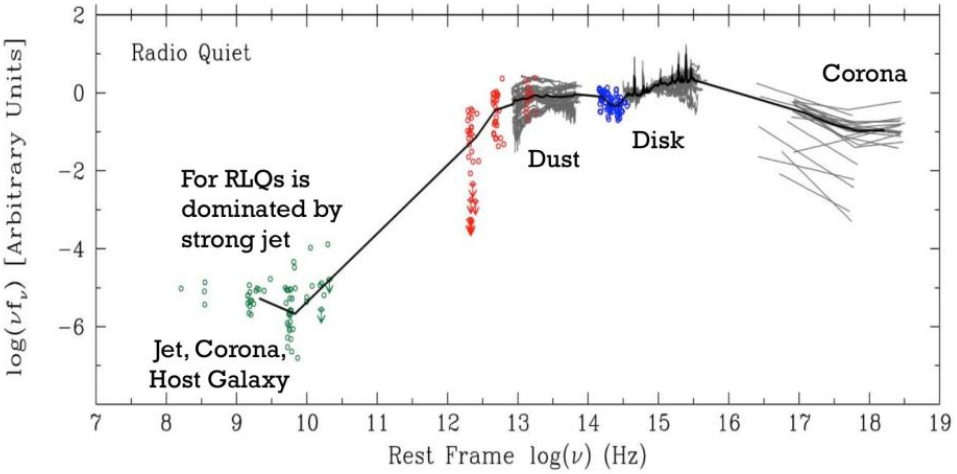

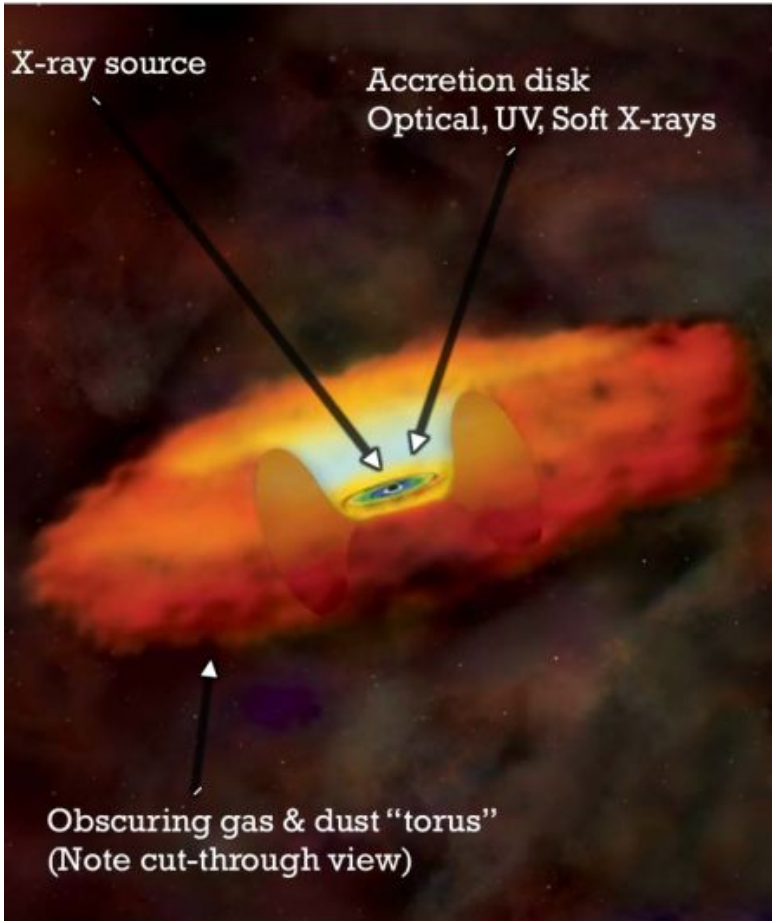

BLACK HOLE + ACCRETION DISK MODEL

AGN Spectral Energy Distribution:

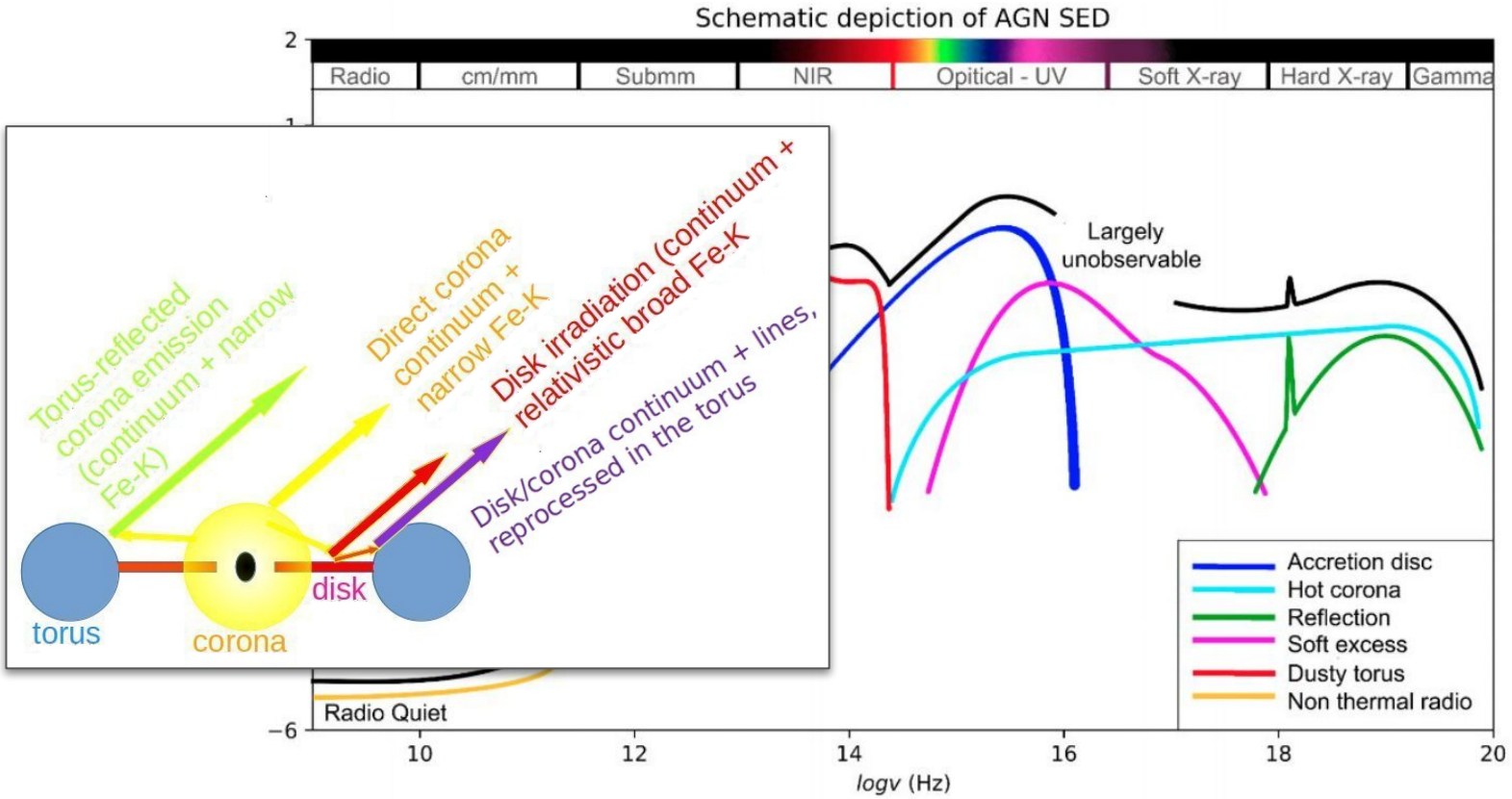

BLACK HOLE + ACCRETION DISK MODEL

AGN variability and accretion disk:

- **AGN variability reflects the radial temperature structure and characteristic timescales of the accretion disk**
  - **Different wavelengths originate at different radii in the disk, and different radii have different physical timescales → That radial stratification *naturally* produces wavelength-dependent variability.**
- **The accretion disk is expected to have about the correct size to explain the observed variability timescales and naturally explains the change in variability as a function of frequency.**

$$\text{Shorter wavelength} \Rightarrow \text{smaller radius} \Rightarrow \text{faster} + \text{stronger variability}$$

$$\text{Longer wavelength} \Rightarrow \text{larger radius} \Rightarrow \text{slower} + \text{weaker variability}$$

- **At a fundamental level, the physical origin of the variations is still poorly understood**
  - **MHD simulations of accretion disks indicate several possible causes of variability: local random variations in dissipation, non-axisymmetric structures, global precession of tilted flows, etc.**

BLACK HOLE + ACCRETION DISK MODEL

Particle Jets:

- **BH accretion is a natural good candidate to fuel particle jets; it provides:**
  - **Enormous energy reservoir with high conversion efficiencies**
  - **Relativistic motions**
  - **Strong, Magnetic fields (also responsible for the X-ray corona emission)**
  - **Rotating compact object → Stable "gyroscope"**

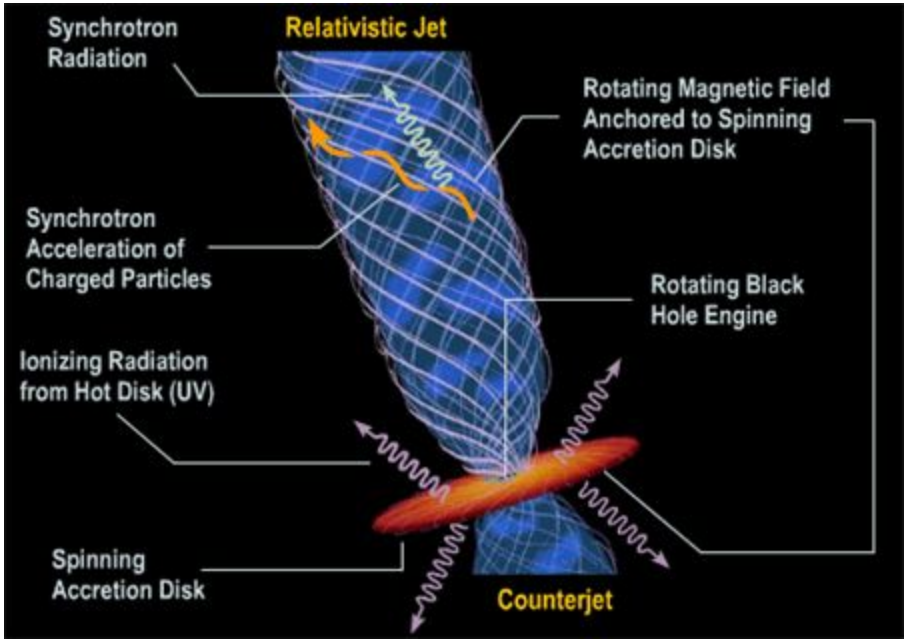

FINDING AGNs: OPTICAL / UV COLORS

AGN detection in the optical/UV:

- **Up to z~2.5, look for point sources brighter in UV than normal starts**
- **At z>2-2.5, absorption by the IGM makes quasars very red in the blue part of the spectrum**
  - **Reddening is problematic; These methods work best for unobscured quasars**
- **For low AGN luminosities, host-galaxy light becomes problematic**

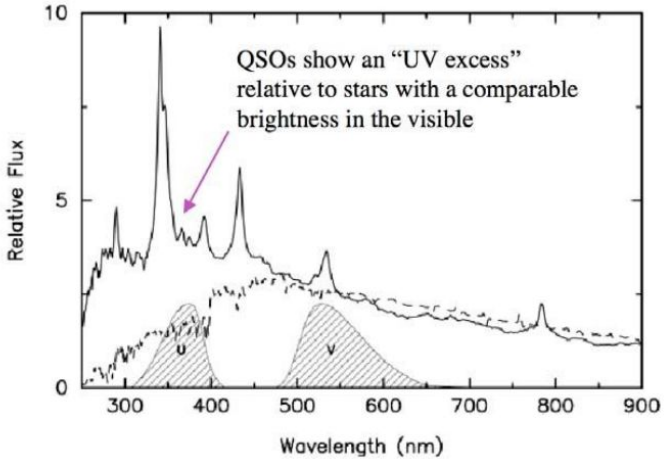

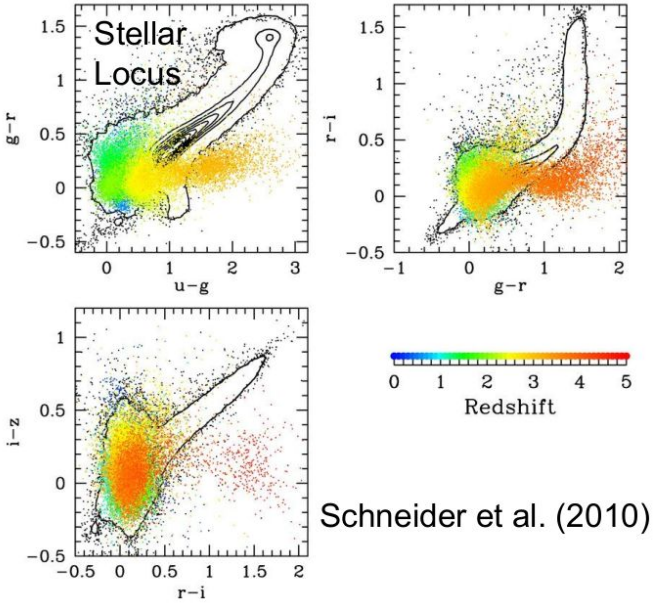

Schneider et al. (2010)

FINDING AGNs: OPTICAL / UV COLORS

AGN detection in the optical/UV:

- **There are many methods for finding AGNs**
- **All methods devised for finding AGNs have limitations and selection effects.**
- **For a complete census, want to apply as many methods as possible enabling cross-checks.**

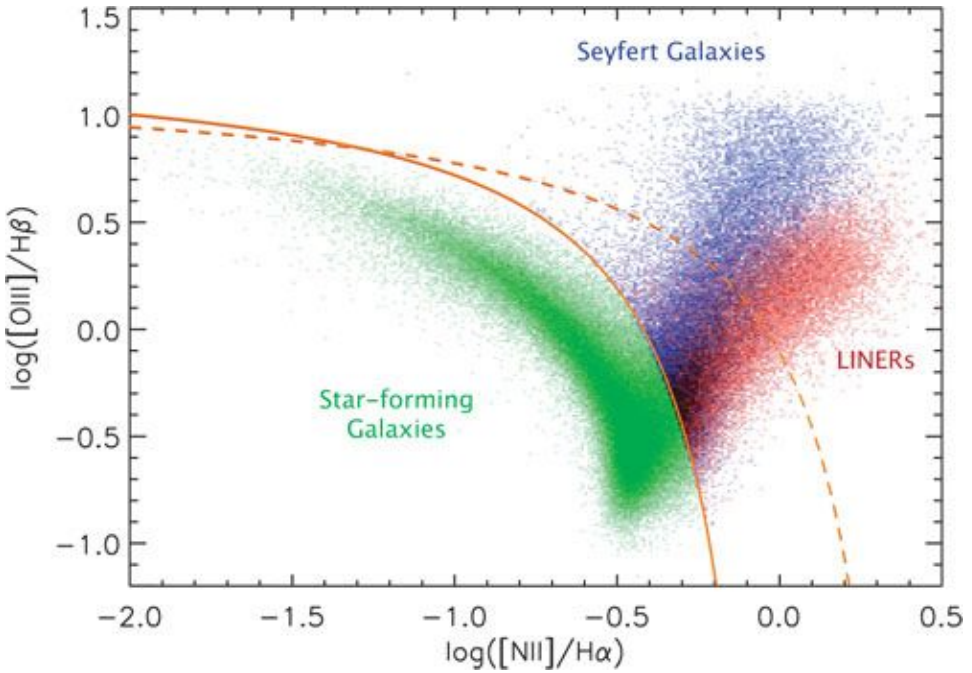

This figure reveals the spread of emission-line galaxies from the Sloan Digital Sky Survey (SDSS) on the line ratio diagnostic diagram of Baldwin, Phillips & Terlevich (1981, PASP, 93, 5). This diagram uses 4 strong optical emission lines, [OIII] 5007A, [NII] 6583A, H-a 6563A, and H-b 4861A, to distinguish galaxies that are dominated by ionization from young stars (labelled "Star-forming Galaxies"), from those that are ionized by an accreting supermassive black hole in the nucleus (Seyfert and LINER galaxies). The curves indicate empirical (solid) and theoretical (dashed) dividing lines between active galactic nuclei (AGN) and star-forming galaxies

FINDING AGNs: OPTICAL / UV COLORS

- The **largest AGN/QSO survey in the optical/UV to date** is the **Sloan Digital Sky Survey (SDSS) quasar catalog** (**SDSS-IV/eBOSS DR16**)
  - **~750,000 spectroscopically confirmed quasars**
  - **Redshift range:** from **z ≈ 0.1 to z ≈ 6**
  - Provides the **largest homogeneous optical AGN sample** for demographics, evolution, and cosmology studies

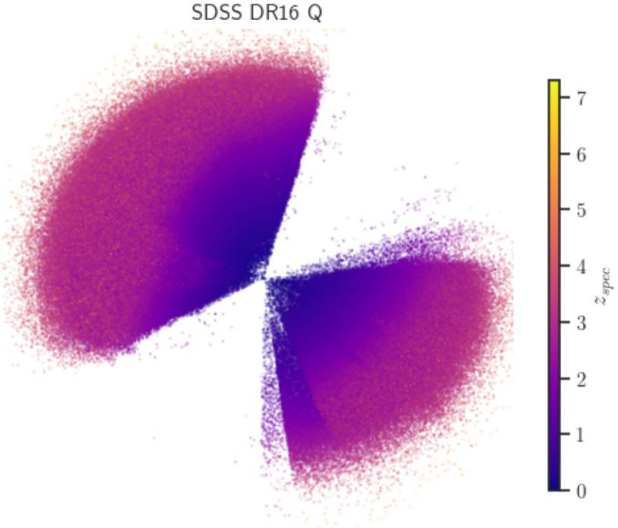

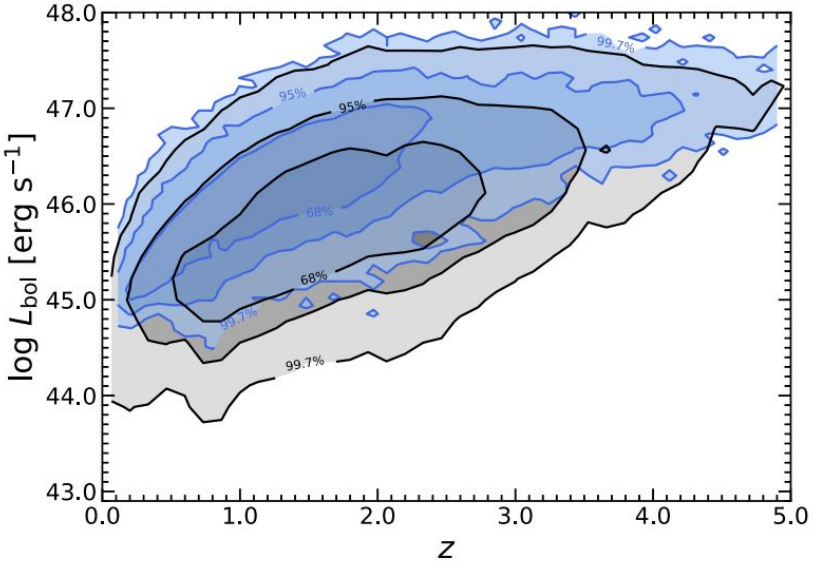

Figure 1. Distribution of quasars in the redshift and luminosity space. The DR16Q sample is shown as black contours. The blue contours are for the SDSS DR7 quasars compiled in Shen et al. (2011). Enclosed percentiles are marked for each contour level.

FINDING AGNs: X-ray

- Almost all AGNs are strong X-ray emitters
- X-ray have reduced absorption bias compared to optical/UV, especially for high-energy X-rays
- In X-ray it is maximized the contrast between black-hole vs. host-galaxy light
- It is easier to find obscured AGNs and lower luminosity AGNs than in optical/UV

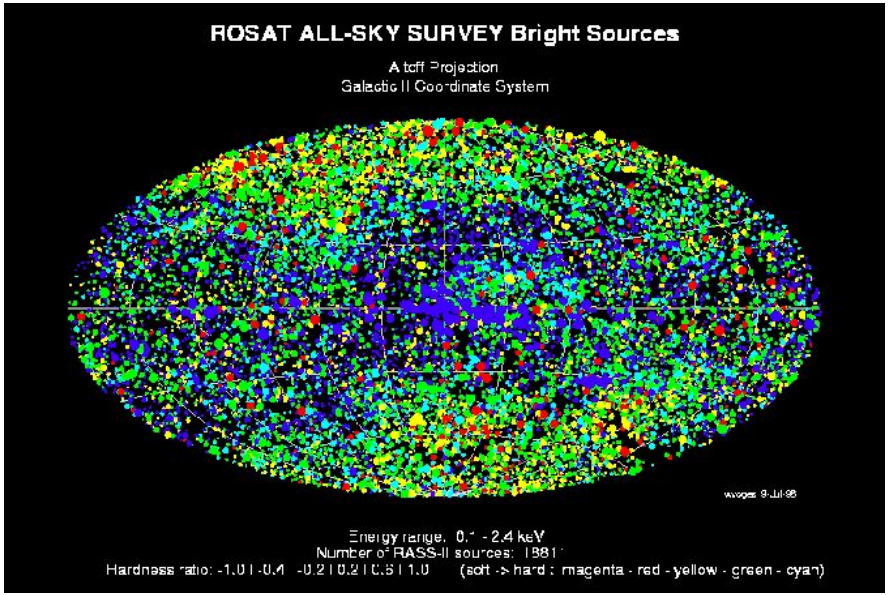

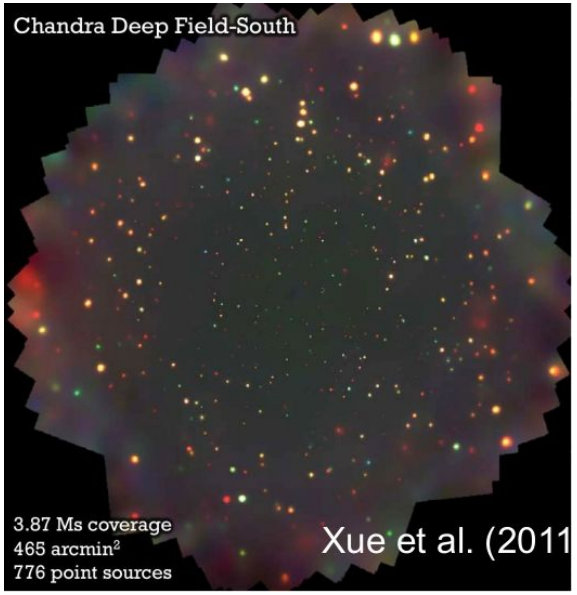

FINDING AGNs: X-ray

- eRosita DR1 (2024) detected nearly 1M sources (resolved ~20% of the CXRB)

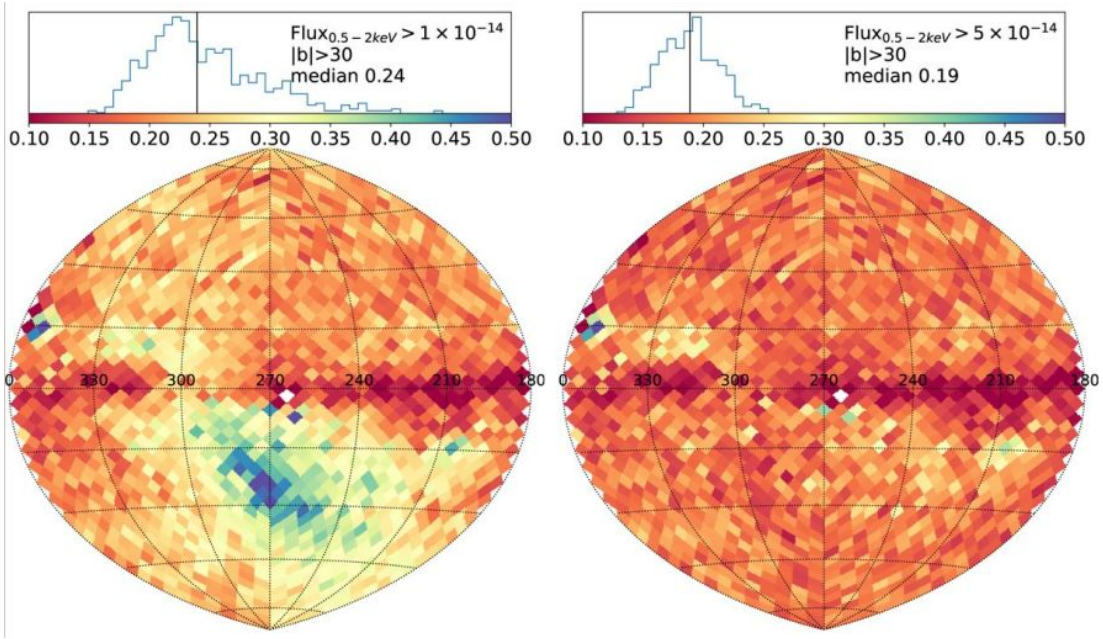

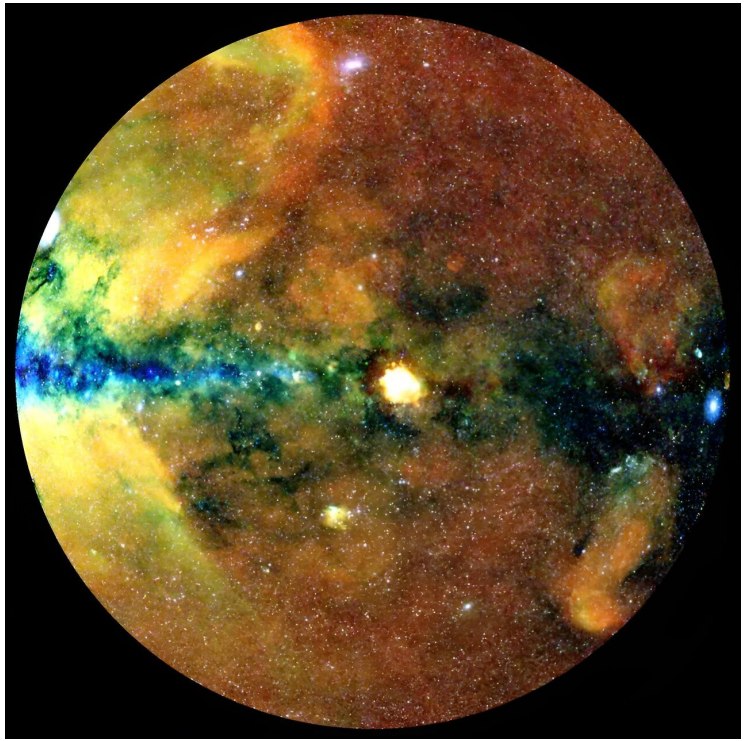

FINDING AGNs: γ-ray

- **AGNs with radio jets pointing toward us (blazars) can be detected in the gamma band.**

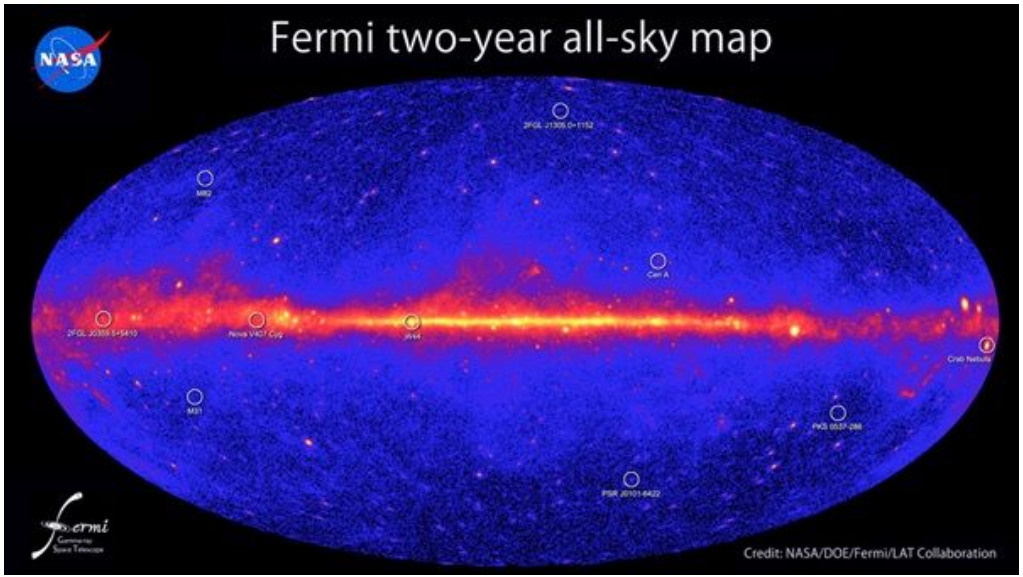

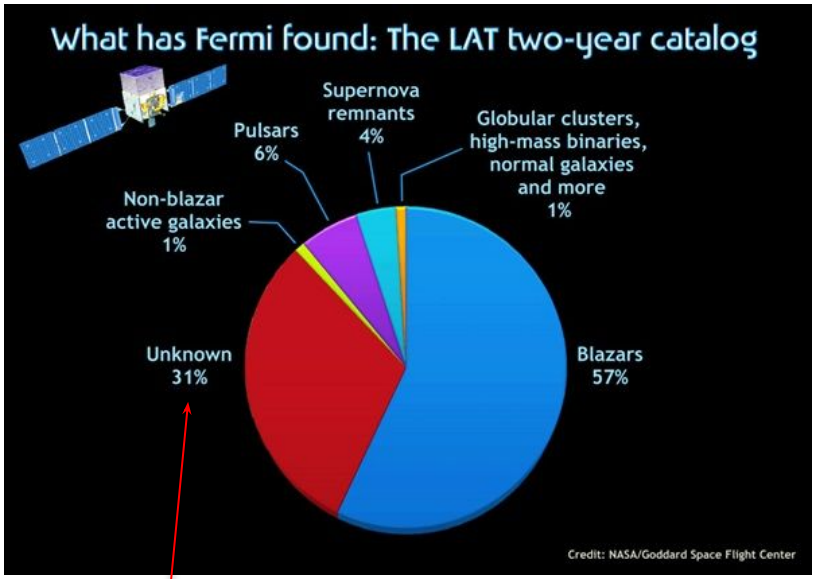

Mostly also AGNs (Blazars) too faint in radio or optical bands to be detected

FINDING AGNs: IR

- Detecting AGN in the infrared (IR) relies on the fact that the accretion disk radiation is absorbed by dust and re-emitted thermally in the IR
- Several methods have been developed for the effective selection of AGNs in sensitive infrared data.
- Often are seeing infrared power-law emission or “waste heat” from the AGN re-emitted by warm dust.
- These are also relatively resistant against obscuration effects.
- They sometimes even find AGNs missed in X-ray surveys.
- At lower AGN luminosities, such surveys suffer substantial contamination from star-forming galaxies.

Method	What you look for	Why it works
MIR colors	Red W1–W2	Hot dust power-law
Spectroscopy	[Ne V], weak PAH	Hard ionizing field
SED fitting	MIR excess	Torus emission
Variability	IR lag	Dust reprocessing

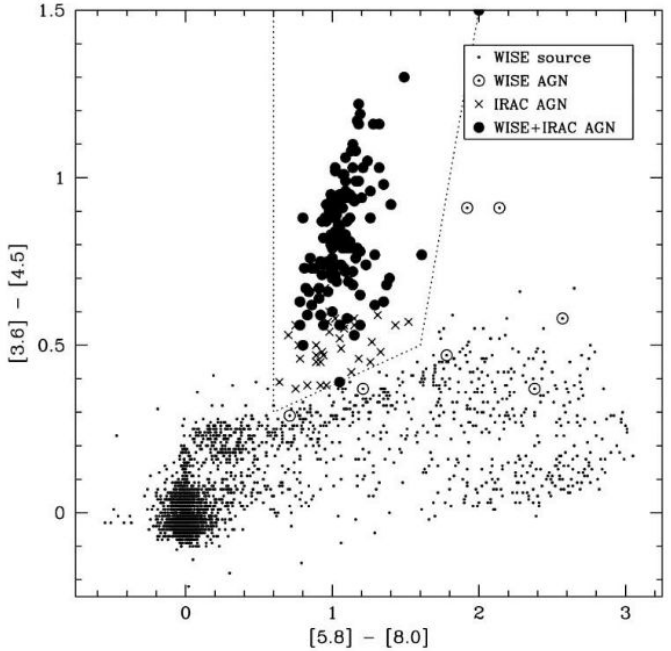

Figure 4. IRAC color–color diagram of *WISE*-selected sources in the COSMOS field. We only plot sources with S/N $\geqslant$ 10 in $W1$ and $W2$, and we require $[3.6] > 11$ to avoid saturated stars. Sources with $W1 - W2 \geqslant 0.8$ are indicated with larger circles; filled circles indicate sources that were also identified as AGNs using the Stern et al. (2005) mid-infrared color criteria. Sources identified as AGNs using *Spitzer* criteria but not using the *WISE* criterion are indicated with ×'s.

Stern et al. (2012)

FINDING AGNs: RADIO

- Detecting AGN in the radio exploits the fact that relativistic jets produce non-thermal synchrotron emission ($L_{@1.4GHz} > 10^{24}$ W /Hz). This radio emission is physically distinct from the thermal processes that dominate normal star-forming galaxies.
- Many of the first quasars were found via radio selection (3C catalog).
- About 10% of AGNs are radio-loud sources.
- Stars are usually very weak radio sources, so little stellar contamination.
- Not affected by dust extinction → can detect heavily obscured AGNs
- AGN radio catalog are often quite incomplete, owing to radio-quietness of many AGNs, but sensitive radio surveys can detect many radio-quiet AGNs too.

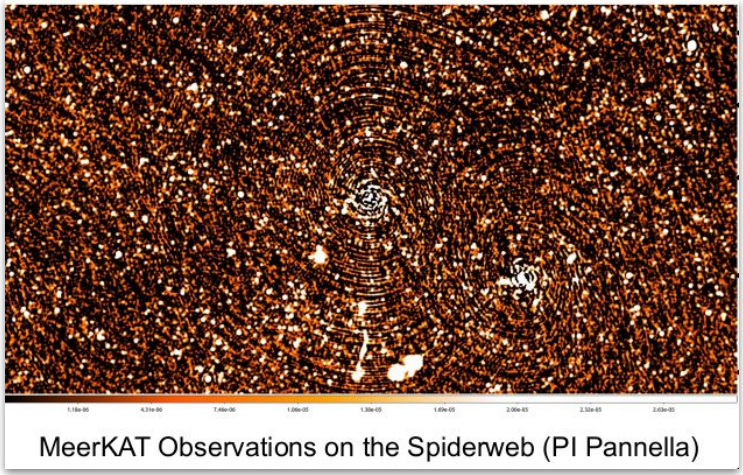

MeerKAT Observations on the Spiderweb (PI Pannella)

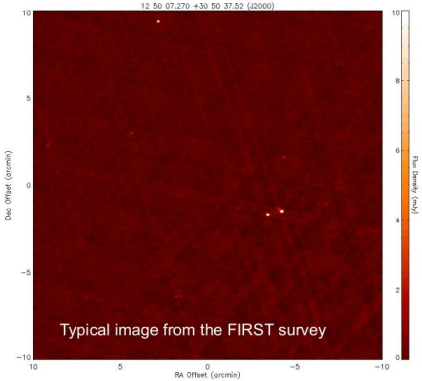

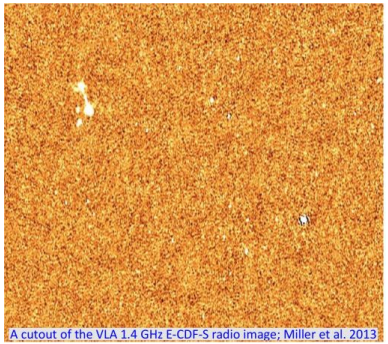

A cutout of the VLA 1.4 GHz E-CDF-S radio image; Miller et al. 2013

FINDING AGNs: RADIO

- Detecting AGN in the radio exploits the fact that relativistic jets produce non-thermal synchrotron emission ($L_{@1.4GHz} > 10^{24}$ W /Hz). This radio emission is physically distinct from the thermal processes that dominate normal star-forming galaxies.
- Many of the first quasars were found via radio selection (3C catalog).
- About 10% of AGNs are radio-loud sources.
- Stars are usually very weak radio sources, so little stellar contamination.
- Not affected by dust extinction → can detect heavily obscured AGNs
- AGN radio catalog are often quite incomplete, owing to radio-quietness of many AGNs, but sensitive radio surveys can detect many radio-quiet AGNs too.
- Often involves “human intervention” → Visual inspection, or nowadays, ML techniques

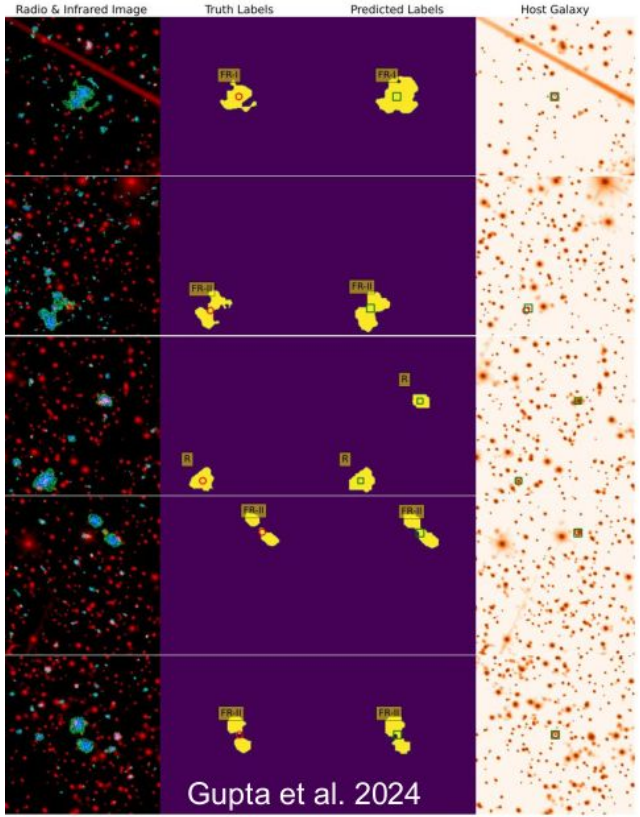

The AGN bestiary

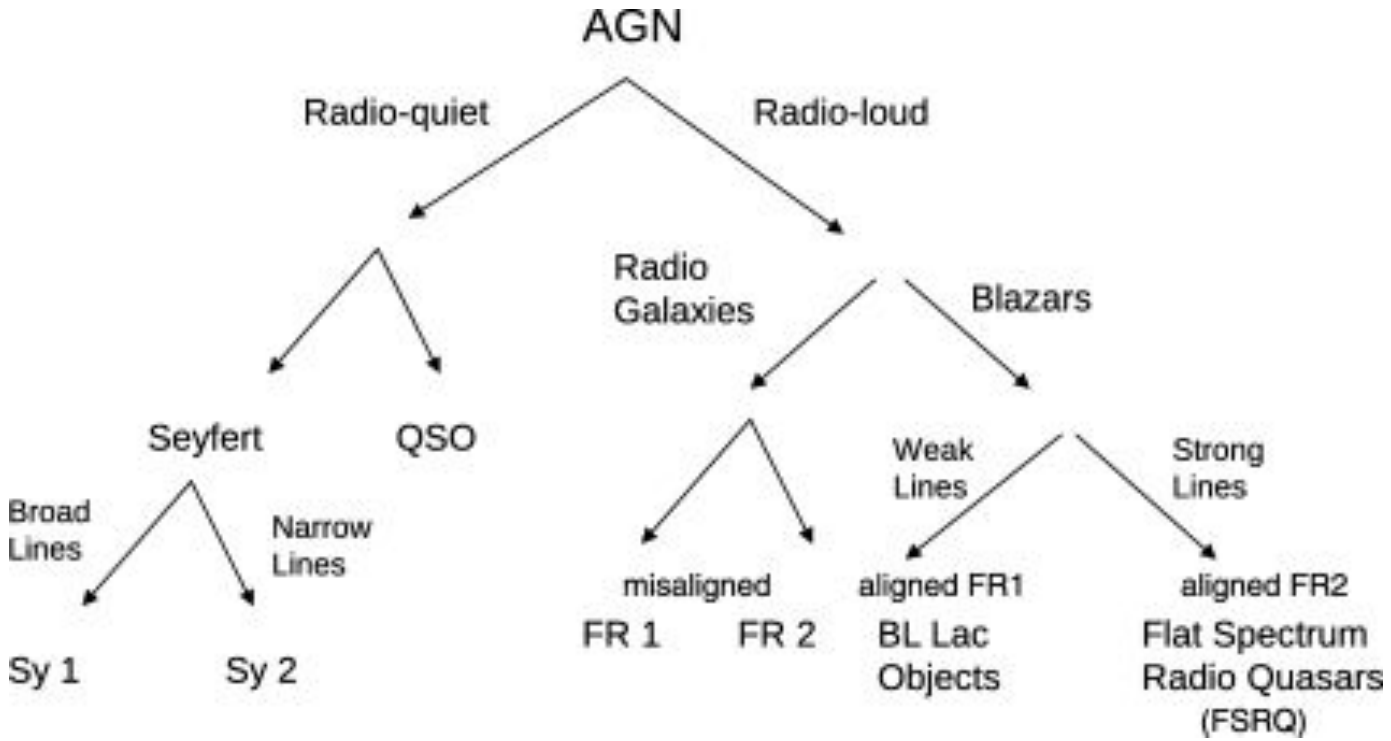

The AGN bestiary: Seyfert galaxies

There are two type of Seyfert galaxy based on the presence of broad emission lines:

- **Seyfert 1 (Sy1):**
  - **~20% of all Sy**
  - **Broad lines (>1000 km/s)**
  - **Strong UV and X continuum**
  - **Luminosity up to ~10^{45} erg/s (~2e11 $L_\odot$)**

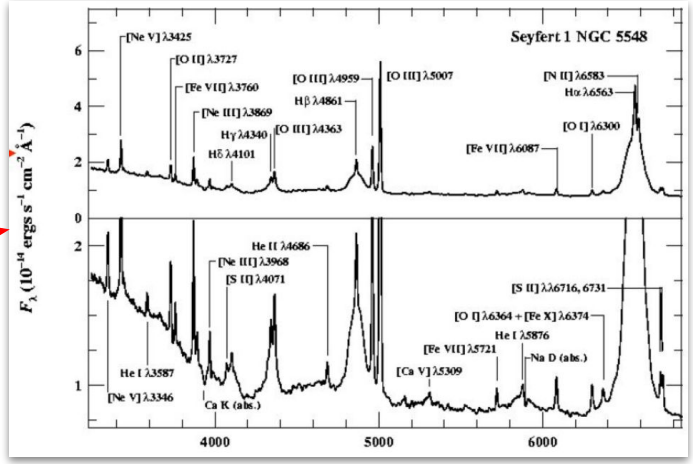

- **Seyfert 2 (Sy2):**
  - **~80% of all Sy**
  - **Only narrow lines (<1000 km/s)**
  - **UV and X continuum weak compared to host galaxy**

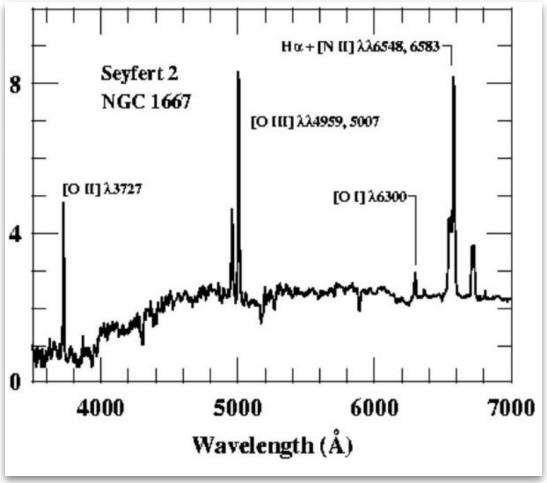

The AGN bestiary: Seyfert galaxies

There are sub-classes of Seyfert galaxies:

- **Sy1.2: Strong broad Balmer components (e.g. Hβ Hα) with a noticeable narrow component "cusp"**
- **Sy1.5: Comparable strengths between the broad and narrow components**
- **Sy1.8: Broad components are very weak, though still detectable in both Hβ and Hα**

- **Narrow Line Seyfert 1 (NLS1):**
  - **Sy1 galaxies with “narrow” broad lines: 1000 km/s < FWHM < 2000 km/s**
- **Low Ionization Narrow Line Region (LINER):**
  - **Analogous to Sy2 but with strong low-ionization lines**

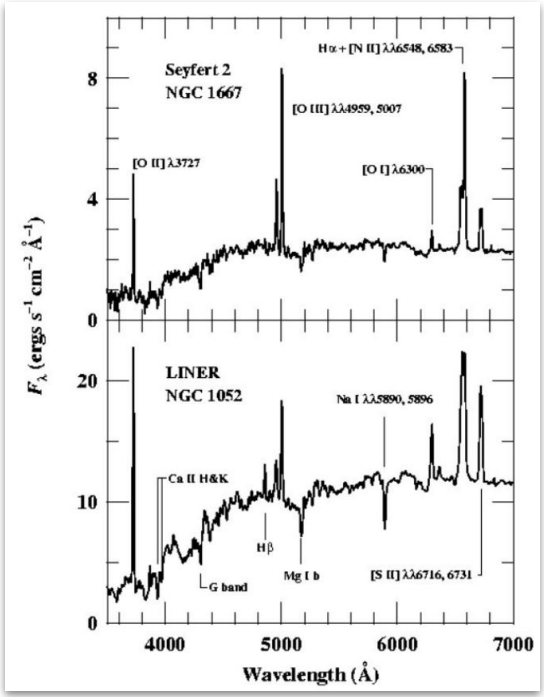

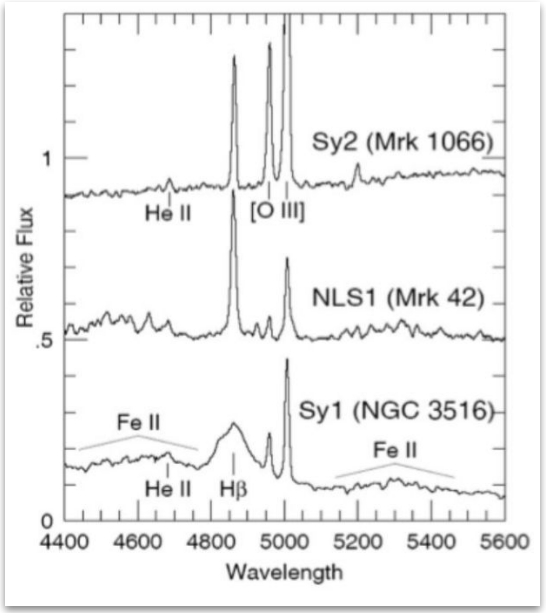

The AGN bestiary: Quasar

- **Discovered in 1960 as radio sources (Quasar = Quasi stellar radio sources)**
- **Most luminous persistent sources in the Universe (L_{Bol} ~ 10^{44} - L^{48} erg/s) radiating near the Eddington limit → High-luminosity end of AGN population**
- **Their luminosity outshines that of the host galaxy, and they appear as point-like sources**

Feature	Type I Quasar	Type II Quasar
Visibility	Unobscured (Direct view)	Obscured (Hidden by dust)
Broad Lines	Present (Fast-moving gas visible)	Absent (Blocked by the torus)
Brightness	Very bright in UV and Visible light	Faint in Visible; bright in Infrared/X-ray

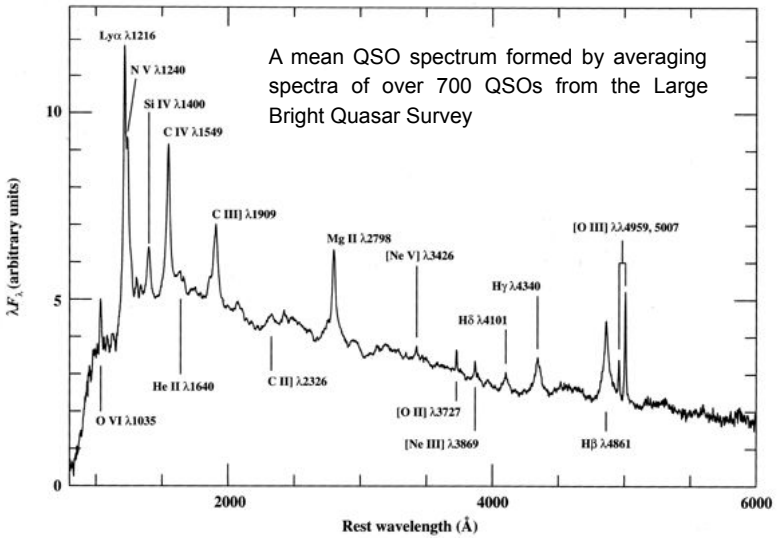

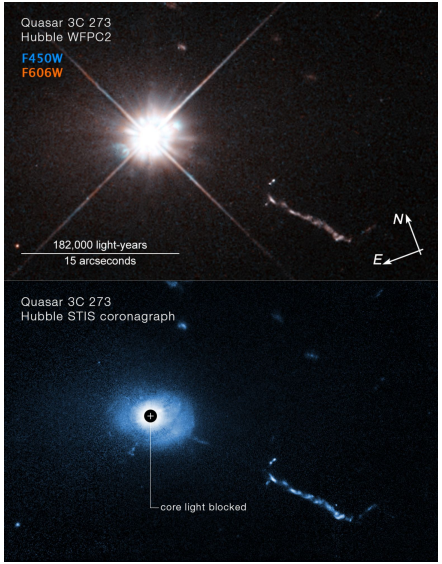

The AGN bestiary: Fanaroff-Riley (FR)

There are two kind of extended radio galaxies classified according to their **radio morphology**:

- **Fanaroff-Riley I:**
  - Brightest near the core
  - Jets fade with distance
  - Diffuse lobes
  - Often in massive ellipticals / clusters
  - Radio power: $L_{1.4GHz} < 10^{24.5}$ W / Hz

- **Fanaroff-Riley II:**
  - Bright terminal hotspots
  - Collimated jets
  - Prominent lobes
  - Often powerful quasars
  - Radio power: $L_{1.4GHz} > 10^{24.5}$ W / Hz

Morphology depends on both intrinsic power and external density (FR II more isolated, high-power jets), not a fundamentally different central engine.

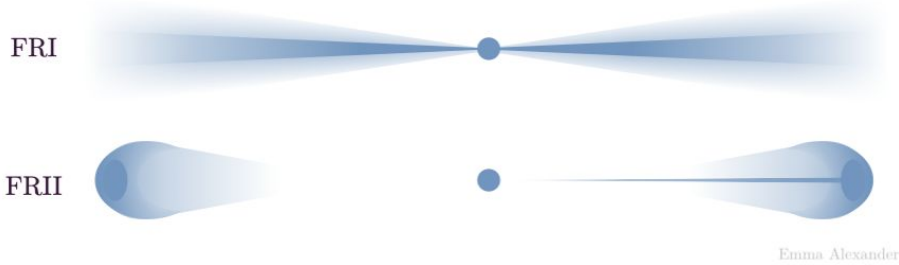

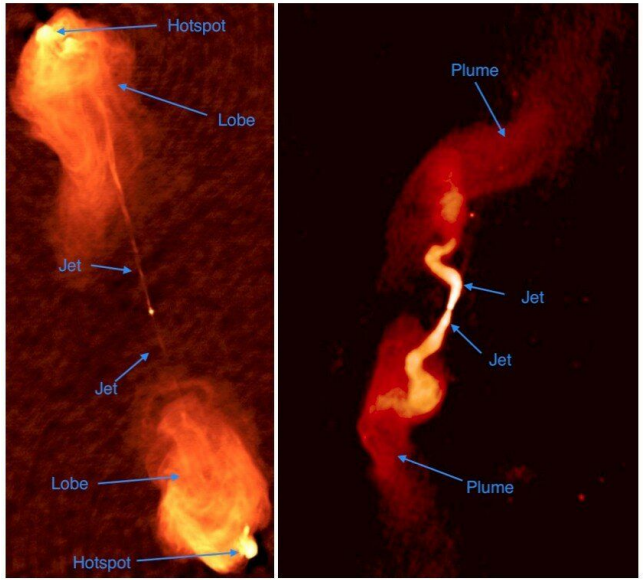

Powerful FR II radio jets in CygnusA (left) and the weak FRI jets in 3C 31 (right) from the VLA (Very Large Array) radio maps.image credit: NRAO/AUI.

The AGN bestiary: Blazar

- **Blazars** are AGN whose jet is aligned close to the LOS
- Characterized by:
  - strong variability (hours to days)
  - high polarization
  - flat radio spectrum
  - apparent superluminal motion
  - Detectable in the γ band
- **BL Lac**: sub-class of blazars characterized by weak or absent emission lines
- **Flat Spectrum Radio Quasars** (FSRQs): sub-class of blazars characterized by strong broad emission lines

The blazar 3C 454.3 lies 7 billion light-years away. VLBA observations detect details less than 100 light-years across in the galaxy's innermost radio jet.

NRAO/AUI/MOJAVE Team/Y. Kovalev

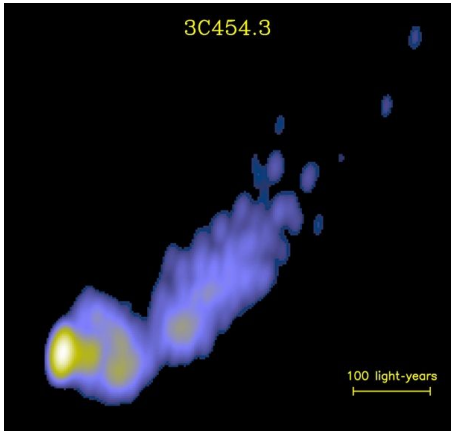

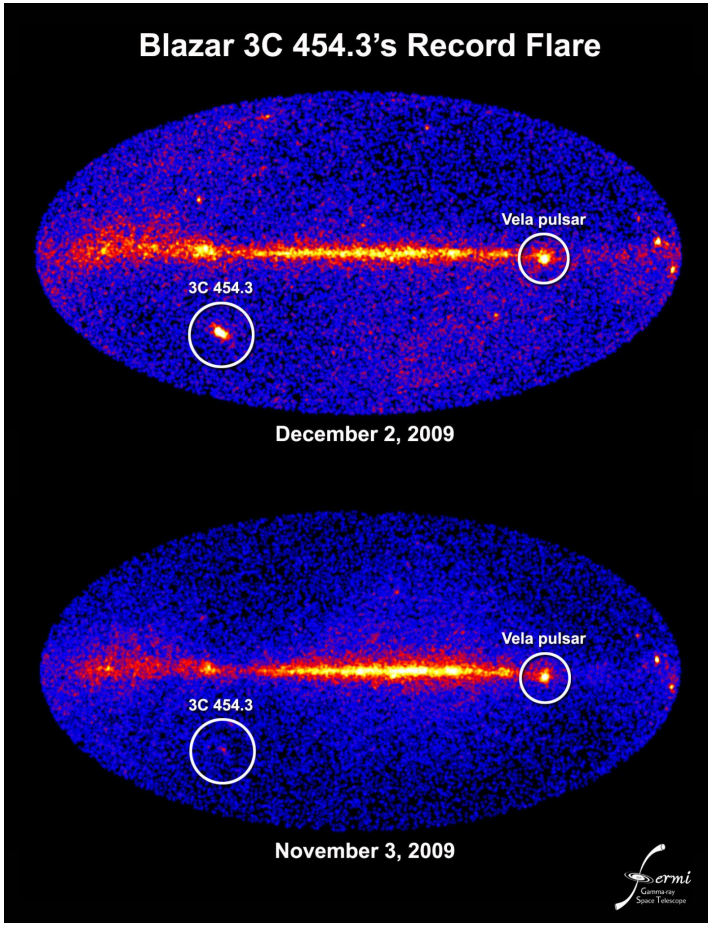

The AGN zoo: Key Classification

- **Strength of Radio Emission**:
  - Radio Loud vs Radio Quiet
- **Optical / UV Emission line properties**:
  - Sy 1 vs Sy 2 galaxy
  - Type 1 Quasar vs Type 2 Quasar
  - Broad Line vs Narrow Line radio galaxy
  - Also intermediate Sy types, NLSy1, BL Lac, etc
- **Variability and UV Absorption Line properties**
- Luminosity is also often used in classifications for largely historical reasons; usually not so fundamental (e.g., Seyferts are just low-luminosity quasars).

Table 1.2: The AGN Bestiary

Beast	Pointlike	Broad-band	Broad Lines	Narrow Lines	Radio	Variable	Polarized
Radio-loud quasars	Yes	Yes	Yes	Yes	Yes	Some	Some
Radio-quiet quasars	Yes	Yes	Yes	Yes	Weak	Weak	Weak
Broad line radio galaxies (FR2 only)	Yes	Yes	Yes	Yes	Yes	Weak	Weak
Narrow line radio galaxies (FR1 and FR2)	No	No	No	Yes	Yes	No	No
OVV quasars	Yes	Yes	Yes	Yes	Yes	Yes	Yes
BL Lac objects	Yes	Yes	No	No	Yes	Yes	Yes
Seyferts type 1	Yes	Yes	Yes	Yes	Weak	Some	Weak
Seyferts type 2	No	Yes	No	Yes	Weak	No	Some
LINERs	No	No	No	Yes	No	No	No

AGN zoo: 3 dimensional classification: optical spectral type, radio properties, and L

	Name	Optical spectral type?	Radio Loud?	Luminosity?
	Seyferts	1, 1.2, 1.5, 1.8, 1.9, 2.0	No	Moderate
	Quasars	1, 2	No	High
	LINERS or low-luminosity AGN	1, 2	Yes and No	Low
Radio sub types	Broad-line Radio Galaxies (BLRGs)	1	Yes	Moderate
	Narrow-line Radio Galaxies (NLRGs)	2	Yes	Moderate
	Radio-loud quasars	1, 2	Yes	High
	FRIs	1	Yes	Low
	FRIIs	1, 2	Yes	Low-High
	Blazars	0!!!	Yes	Low-High

THE UNIFYING MODEL

- A crucial development in understanding Seyfert galaxies (and AGNs) came with the recognition that at least some type 2 Seyfert nuclei are in fact type 1 objects for which our view of the innermost region is blocked by a dust- and gas-rich obscuring torus.
- The key observations involved measurements of polarization. Polarized light enhance the presence of broad lines
    - BL in intensity are ~100 times fainter than continuum and NL, and thus impossible to detect

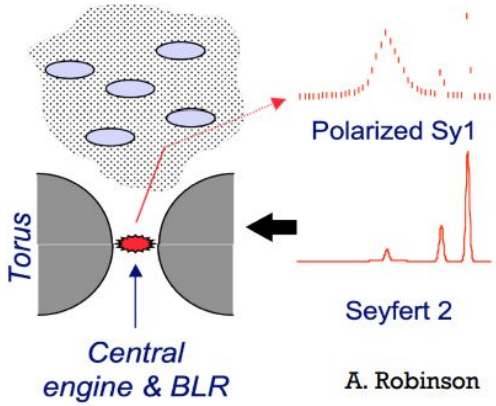

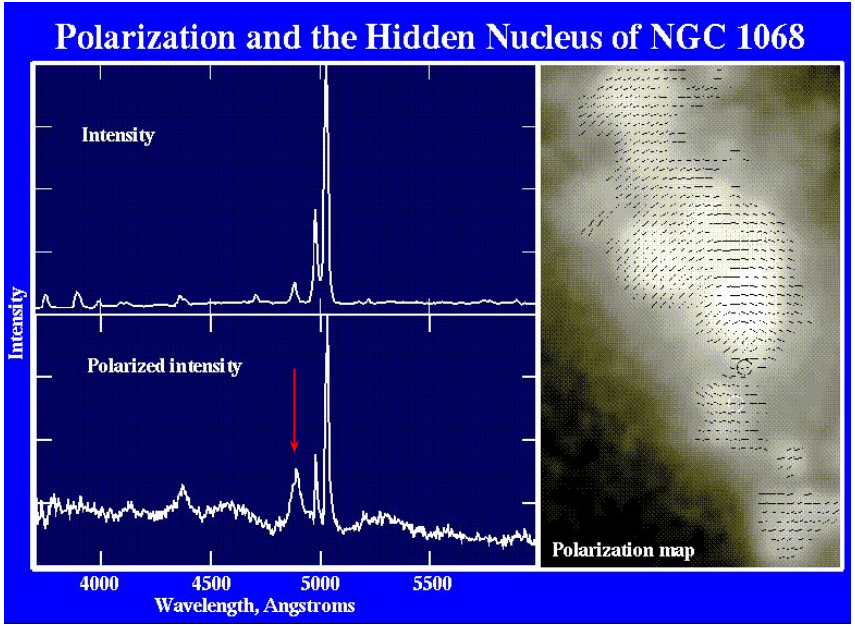

THE UNIFIED MODEL

Unified model: The diversity of observed AGN phenomenology is primarily due to orientation effects relative to an axisymmetric central engine, rather than intrinsic physical differences.

Central Structure (parsec scale)

- **Supermassive black hole (SMBH)**
- **Accretion disk** - thermal UV/optical continuum
- **Broad Line Region (BLR)** - high-velocity gas, Doppler-broadened permitted lines
- **Dusty torus** - optically thick, obscures central regions at high inclination
- **Narrow Line Region (NLR)** - extended, low-density gas, narrow forbidden lines
- **Relativistic jets** (in radio-loud systems)

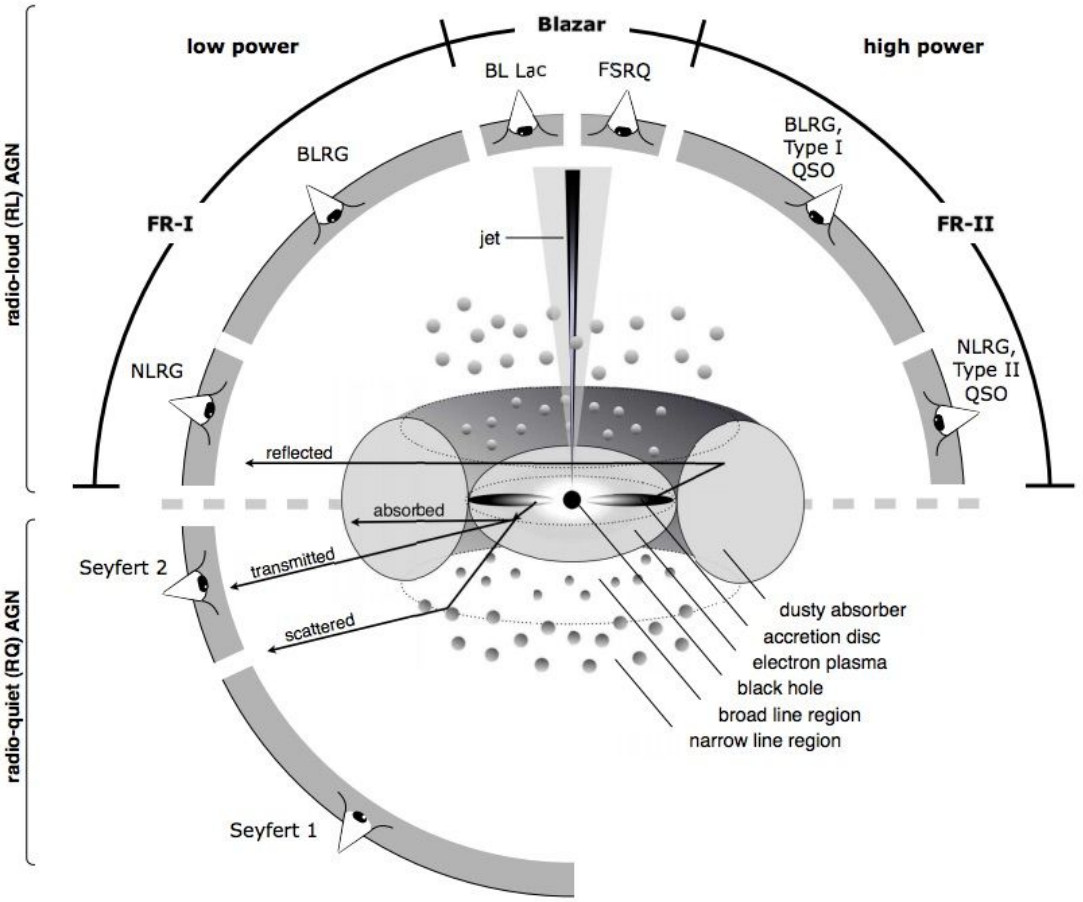

THE UNIFIED MODEL

Unified model: The diversity of observed AGN phenomenology is primarily due to orientation effects relative to an axisymmetric central engine, rather than intrinsic physical differences.

Central Structure (parsec scale)

- **Supermassive black hole (SMBH)**
- **Accretion disk** - thermal UV/optical continuum
- **Broad Line Region (BLR)** - high-velocity gas, Doppler-broadened permitted lines
- **Dusty torus** - optically thick, obscures central regions at high inclination
- **Narrow Line Region (NLR)** - extended, low-density gas, narrow forbidden lines
- **Relativistic jets** (in radio-loud systems)

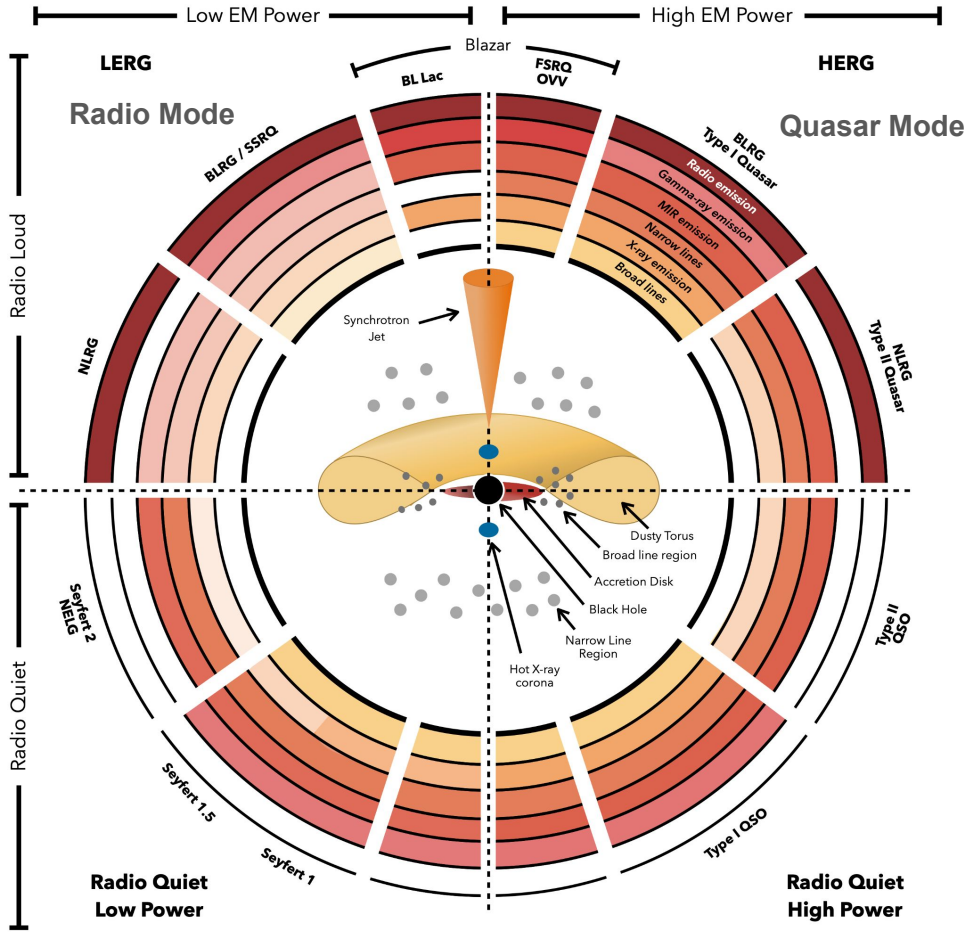

https://publish.obsidian.md/astrowiki/D.+Compact+Objects+%26+Gravitational+Waves/Active+Galactic+Nuclei

THE UNIFIED MODEL

- low and high excitation radio galaxies (LERG/HERG)
- broad line radio galaxy (BLRG)
- narrow line radio galaxy (NLRG)
- narrow emission line galaxy (NELG)
- flat spectrum radio quasar (FSRQ)
- steep spectrum radio quasar (SSRQ)
- optically violent variables (OVV)
- quasi-stellar objects (QSO)

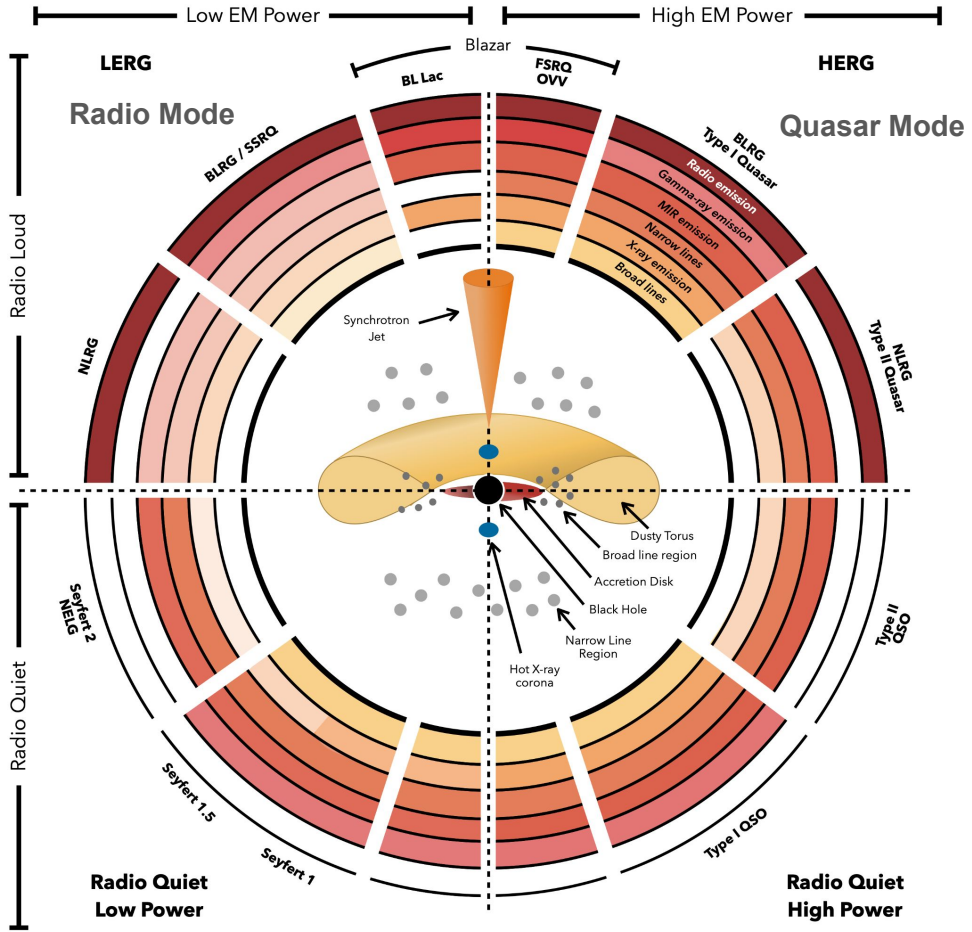

https://publish.obsidian.md/astrowiki/D.+Compact+Objects+%26+Gravitational+Waves/Active+Galactic+Nuclei

THE UNIFIED MODEL

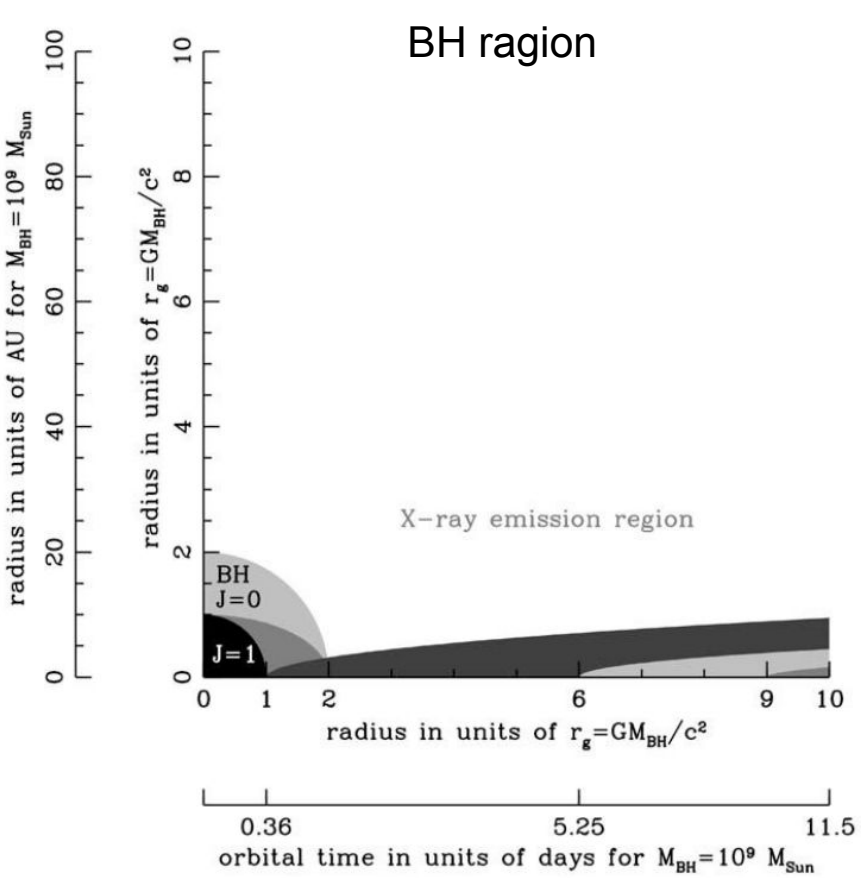

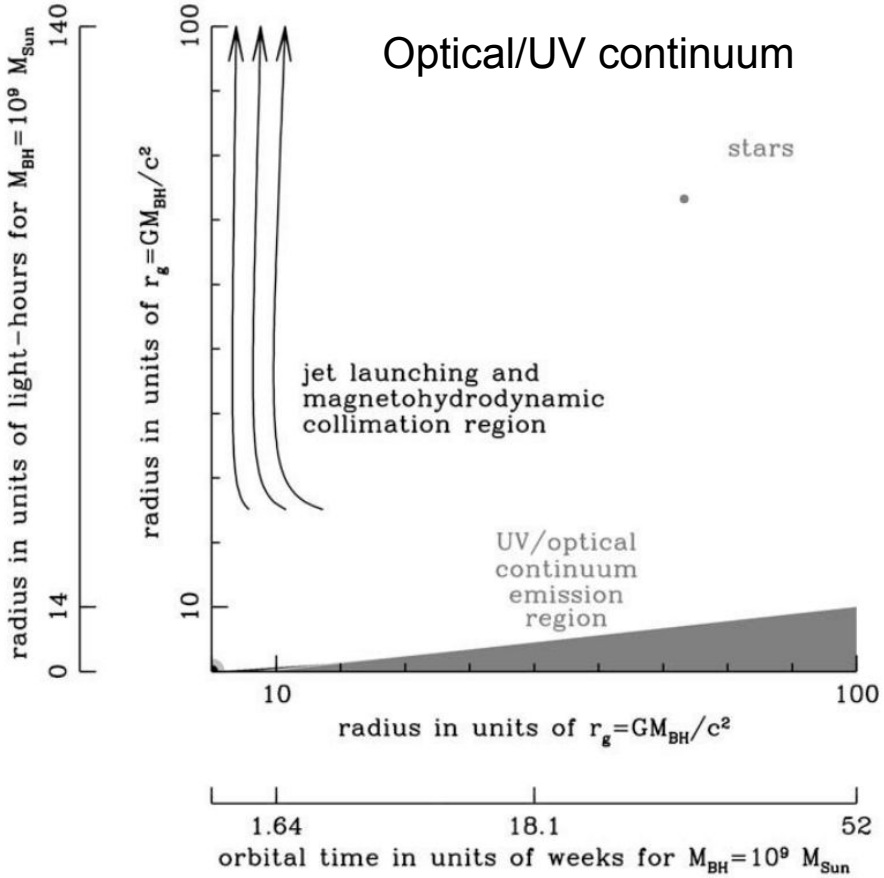

THE UNIFIED MODEL

Broad Line Region

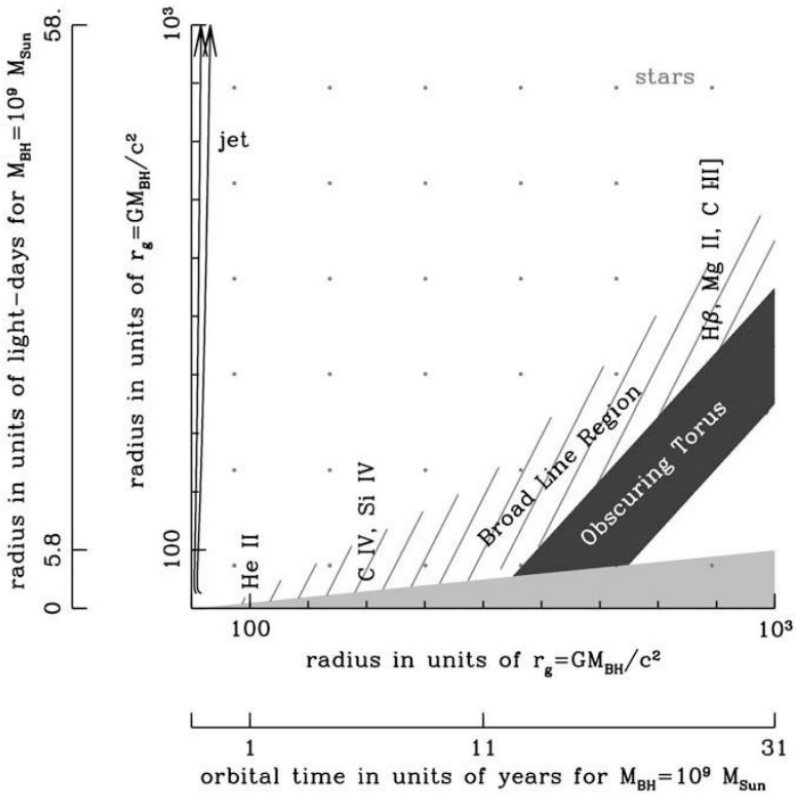

Outflow Region

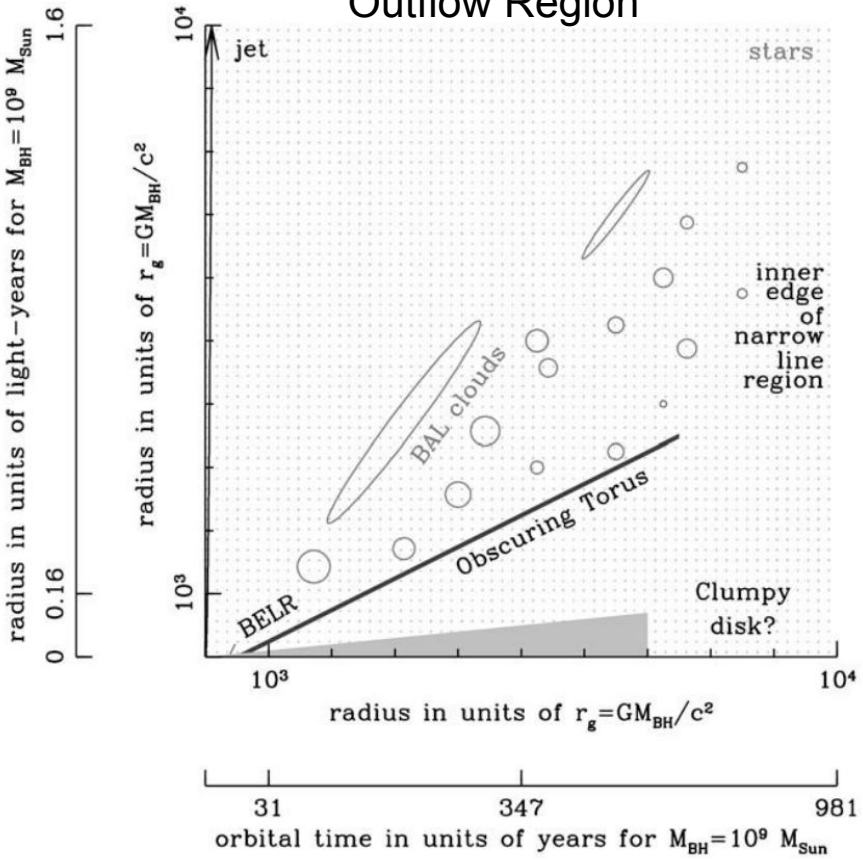

THE UNIFIED MODEL: BH region

Inner ~50 R_s

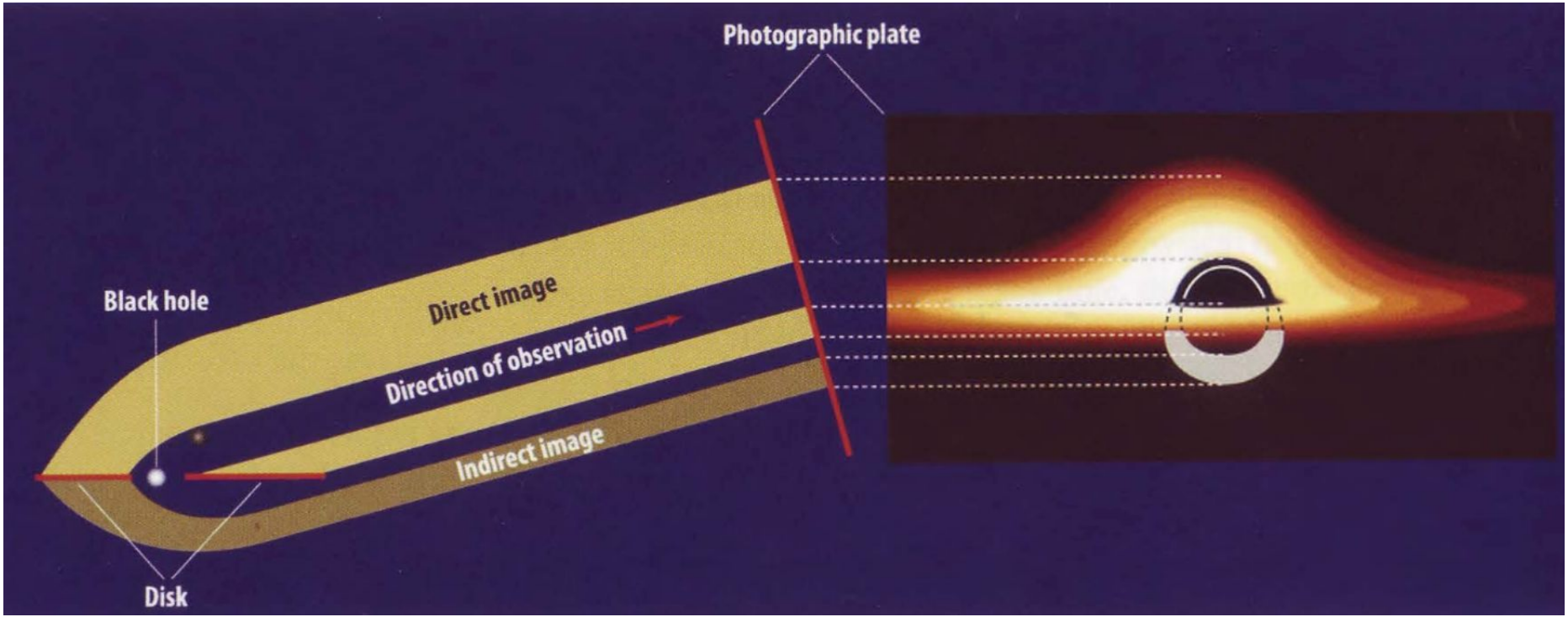

Luminet (1979)

THE UNIFIED MODEL: BH region

Inner ~50 R_s

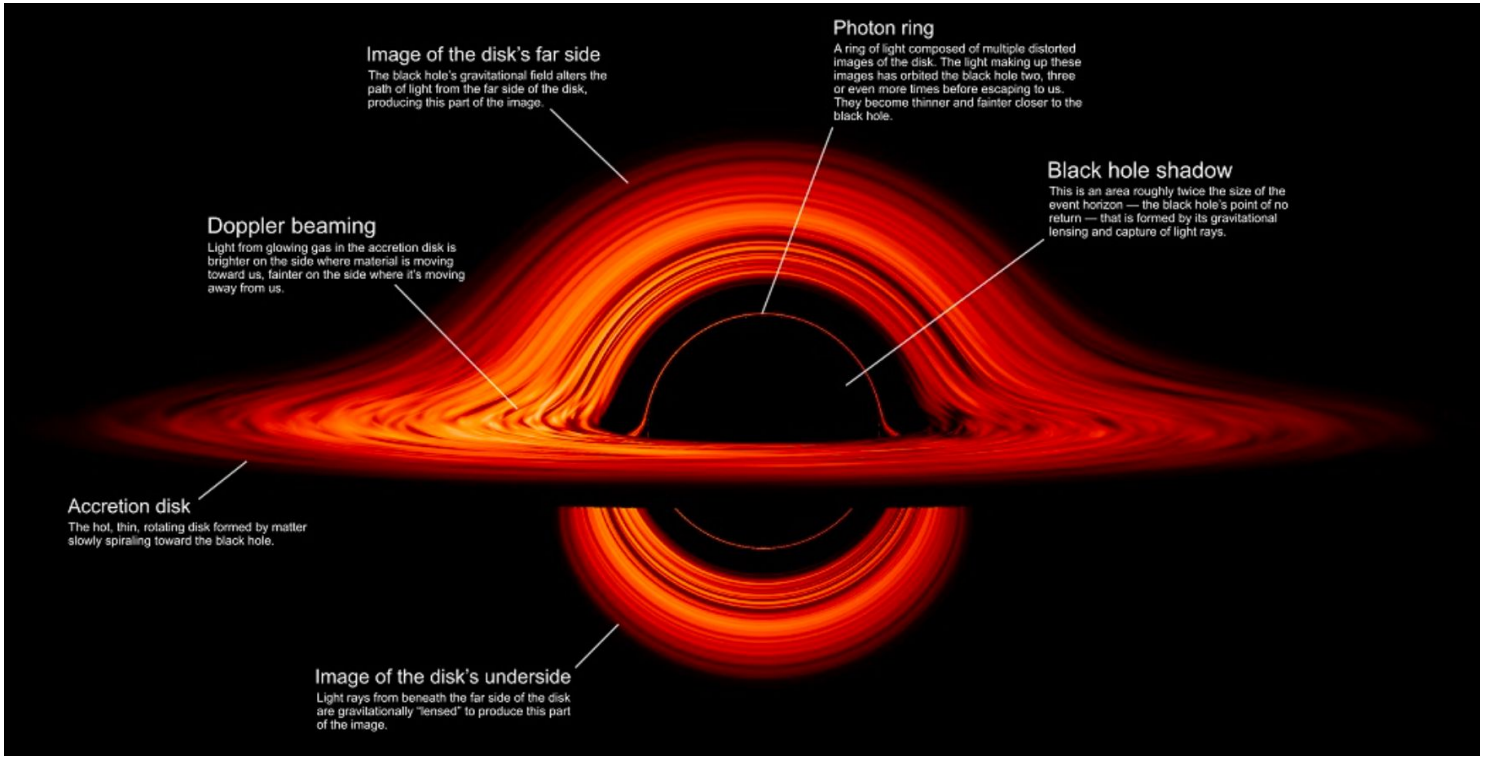

THE UNIFIED MODEL: BH region

- **Almost all AGNs show some X-ray emission**

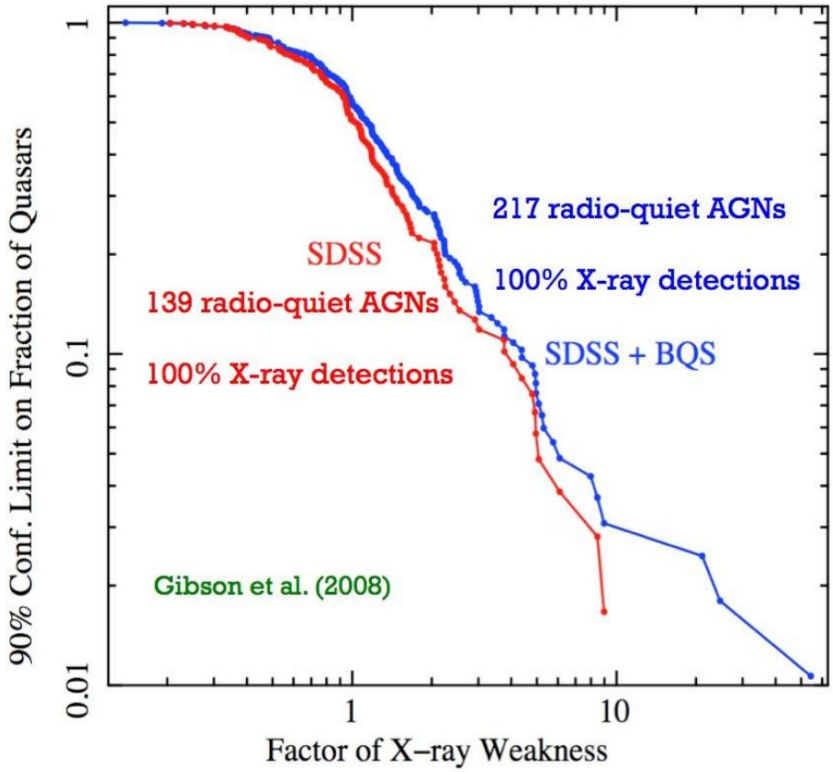

THE UNIFIED MODEL: BH region

X-ray SED:

Continuum components:

- **Power law**
- **Soft X-ray excess**
- **Compton reflection hump**

Discrete atomic features

- **Iron Kα line ~6.4 keV**
- **Other emission lines**

Schematic AGN X-ray Spectral Energy Distribution

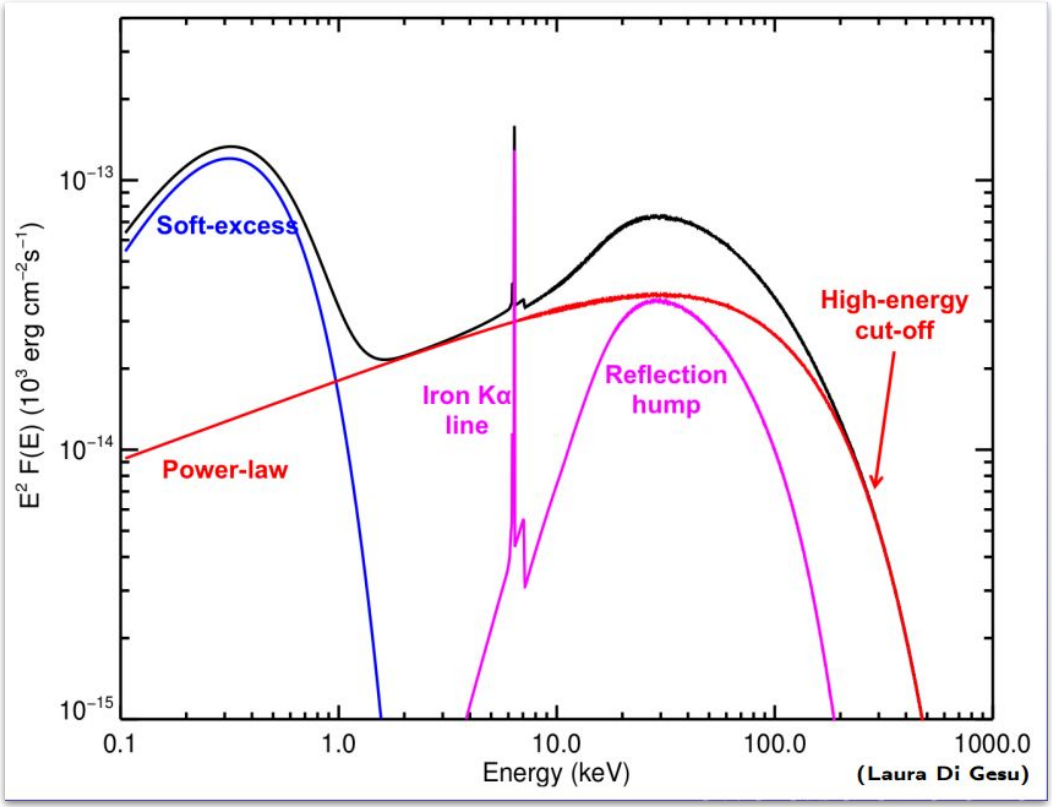

THE UNIFIED MODEL: BH region

X-ray power law continuum:

- **The “corona” Compton up-scatters UV/optical photons from the disk to create the power law continuum**
- **Corona has a temperature of ~100-150 keV.**
- **The high-energy cut-off reflects the maximum energy electrons can transfer (thermal Comptonization)**
- **Corona is likely heated by magnetic flares**
- **The corona’s properties cannot yet be computed from first principle, but progress being made**
- **The corona’s nature remains uncertain:**
  - **Sandwiching the disk?**
  - **Base of a jet?**
  - **Spherical or toroidal?**

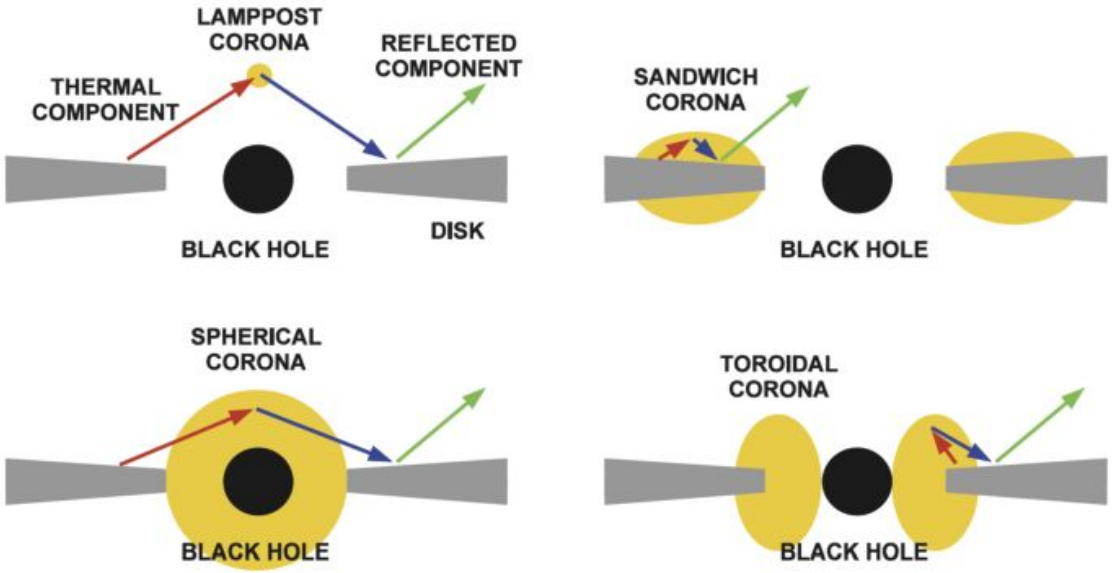

THE UNIFIED MODEL: BH region

Soft X-ray excess:

- **Strong soft X-ray emission (E<1.5 keV) of a ~ blackbody spectral form seen from some objects**
- **Too hot and too variable to be entirely from standard accretion disk (T_{disk}~10eV).**
- **Warm Comptonization: UV disk photons up-scattered by a warm, optically thick Comptonizing corona above the accretion disk (kT_e~0.1 - 1 keV)**
- **Relativistic Blurred Reflection: Emission lines produced in the inner part of the ionized disk are blurred by the proximity of the SMBH by strong Doppler and relativistic effects**

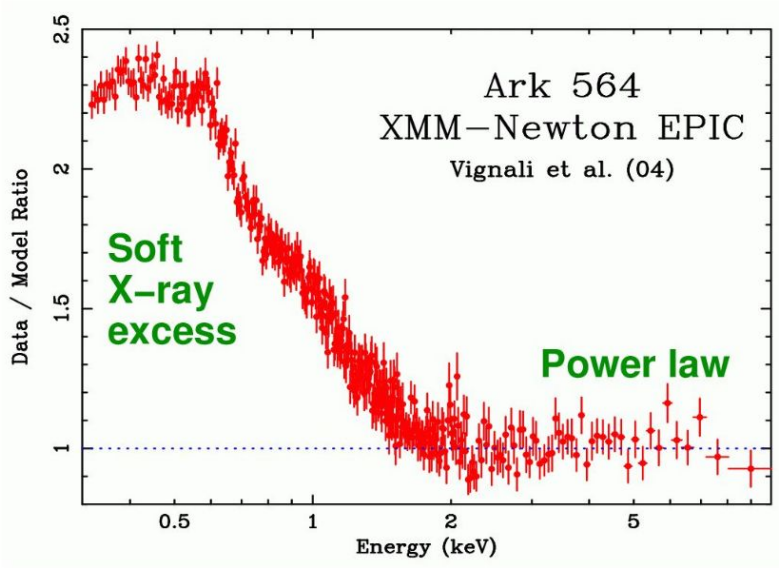

Two-corona model

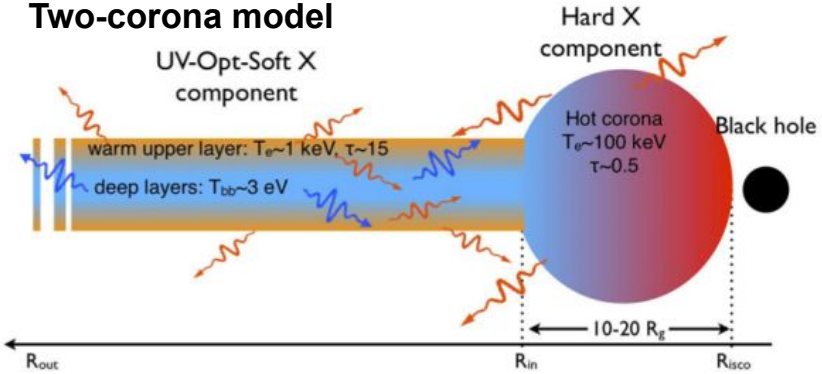

THE UNIFIED MODEL: BH region

Compton Reflection Hump:

- **Broad excess in AGN spectra at E~ 20 -40 keV**
- **Produced by hard X-ray from the hot corona irradiating optically thick material (accretion disk and torus)**
- **Physical interpretation:**
  - **photoelectric absorption suppress soft X-ray (E<15 keV)**
  - **Compton scattering redistributes hard X-ray**
  - **Energy-dependent opacity produces the hump: very high-energy photons penetrate deeply or escape the material, while 20-40 keV photons are efficiently backscattered**

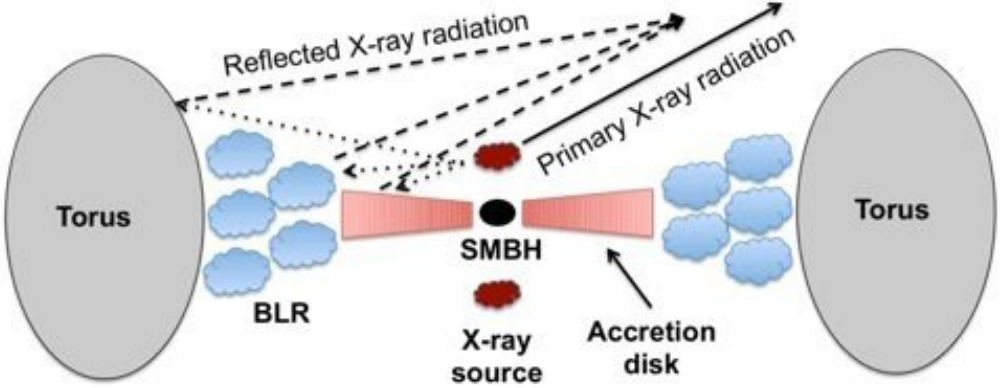

Credit: https://www.astro.unige.ch/~ricci/Website/AGN_in_the_X-ray_band.html

THE UNIFIED MODEL: BH region

Iron Kα Line (6.4 keV):

- **Iron fluorescent emission line produced by hard X-ray from the hot corona irradiating optically thick material (accretion disk and torus)**
- **If produced in inner disk the line is affected by: Doppler broadening, gravitational redshift, light blending → Skewed profile, extended red wing**
- **Kα lines can be use to estimate disk inclination, disk emissivity, and black-hole spin**

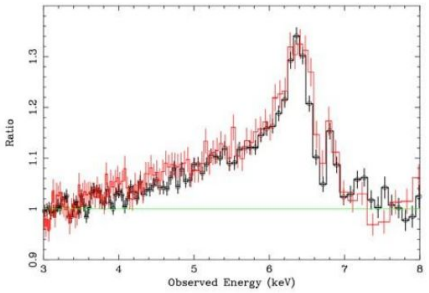

Figure 4: The figure above shows the relativistic disk line profile revealed in MCG-6-30-15 after fitting for the continuum. (Adapted from Miniutti et al. 2007 and Reeves et al. 2006.) The line in MCG-6-30-15 is the best example known presently, and these spectra above are the best yet obtained. The spectrum in black was obtained with *Suzaku*, and the spectrum in red was obtained with *XMM-Newton*.

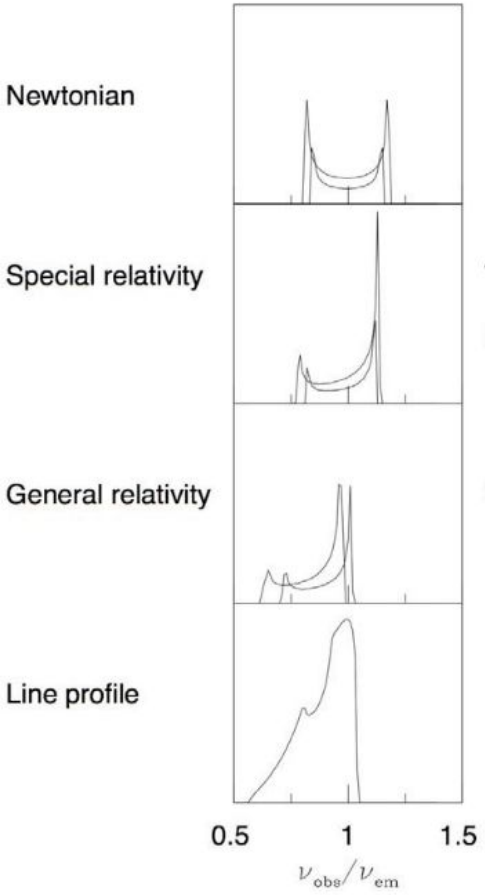

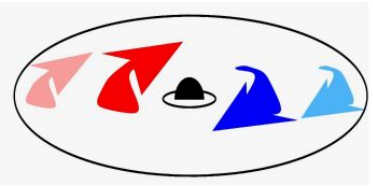

Transverse Doppler shift

Beaming

Gravitational redshift

The relativistic line profile depends on:

- inner disc radius
- inclination of the disc
- emissivity profile

- Fabian et al. (2000)

THE UNIFIED MODEL: BH region

X-ray variability:

- **AGN light curves usually do not show periodicity or quasi-periodicity.**
- **To characterize the variability we compute the power spectral density of the light curve → how variability power is distributed according to timescales**
- **The PSD is characterized by a broken power law. The characteristic timescale of the break is between 0.1-100 days**
- **The break corresponds to a characteristic physical timescale on the accretion flow**
- **The break frequency scales with BH mass → independent BH mass proxy**

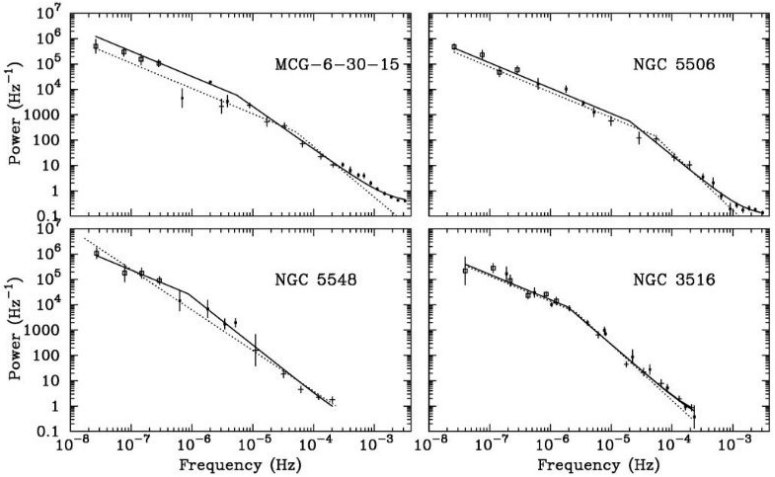

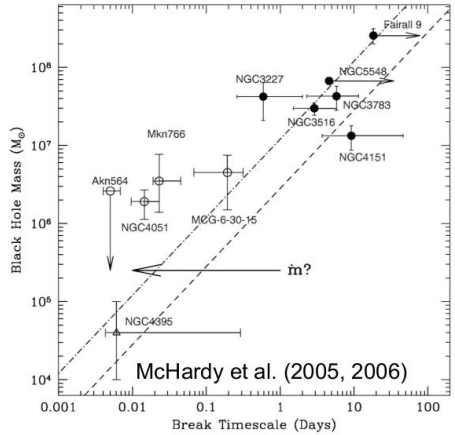

McHardy et al. (2005, 2006)

THE UNIFIED MODEL: Broad Line Region

BLR:

- **Relative strengths of emission lines in AGN spectra indicate we are observing gas in photoionization equilibrium at ~ 10^4K.**
- **Abundances about solar or slightly supersolar**
- **Broad component:**
  - **Doppler widths of 1000-25000 km/s → due to supersonic bulk motion**
  - **Variable on short timescale (days)**
  - **Gas with density n_e~10^9 - 10^{11} cm^{-3} (as determined from strengths /missing of certain density sensitive lines like [O III] and C III])**
- **Arise deeper in the gravitational potential of the AGN**
- **High-resolution spectra reveal a "smooth" broad line profile, suggesting a continuous flow of material, rather than "cloud" structures**

BL are common to AGNs, independently on luminosity and redshift

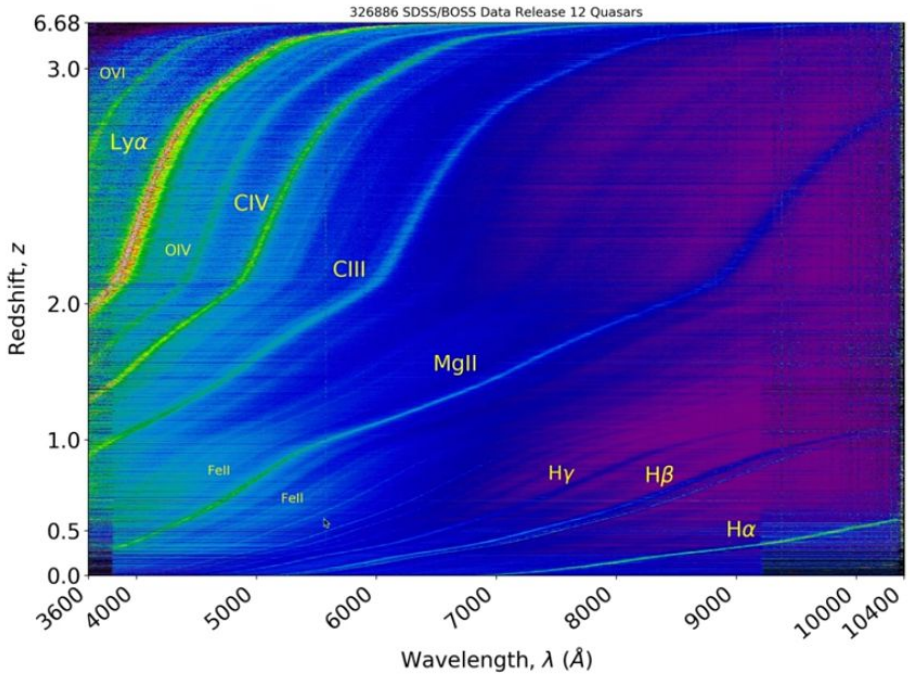

THE UNIFIED MODEL: Broad Line Region

BLR:

- **The broad lines vary on short timescales, usually following the continuum variations with a time delay.**
- **The dime delay is due to the light travel time across the BLR**
  - **Reverberation mapping technique to measure the BLR size → 5 - 500 light days, depending on luminosity**

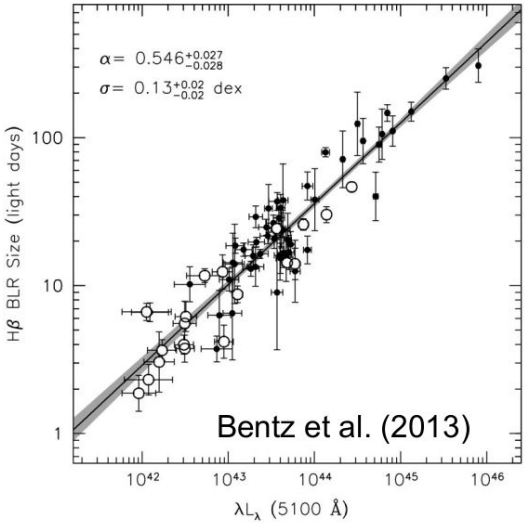

- **The BLR radius is found to scale as $R_{BLR} \sim L^{0.5\text{-}0.7}$**
- **The slope of the relation is about as expected if all AGNs have similar ionization parameters and densities in their BLRs:**

Ionization parameter: $\xi \propto L/nR^2$

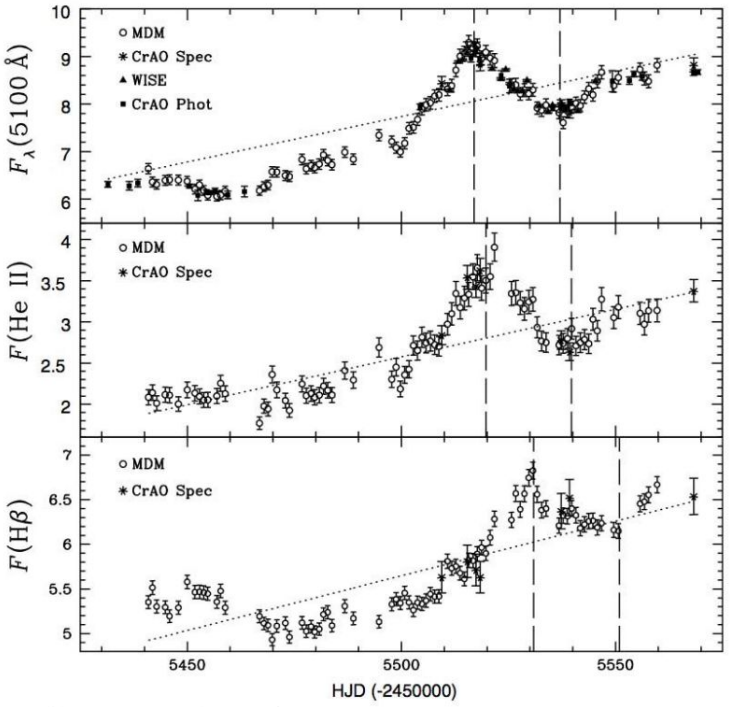

Grier et al. (2012)

THE UNIFIED MODEL: Stratification and virialization

- Reverberation lags have now been measured for several 100s AGNs.
  - The current sample is biased toward AGNs with relatively strong lines.
  - Mostly measured for Hβ , but in some cases for multiple lines.
- The highest ionization emission lines respond most rapidly to continuum changes, indicating ionization stratification.

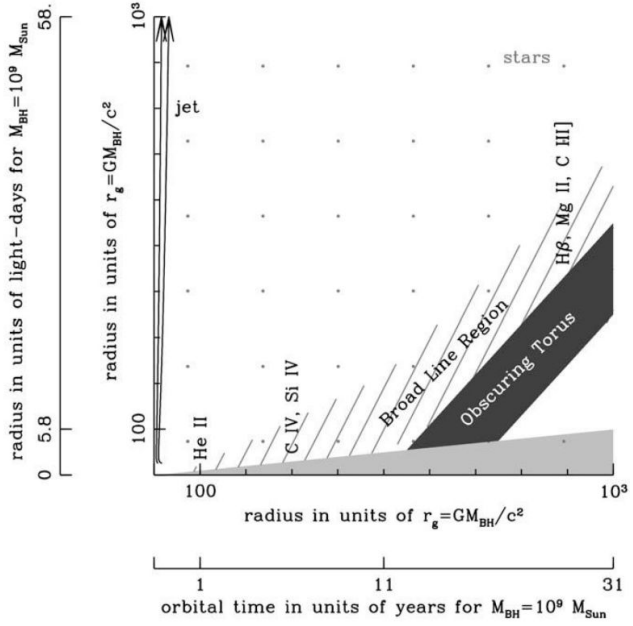

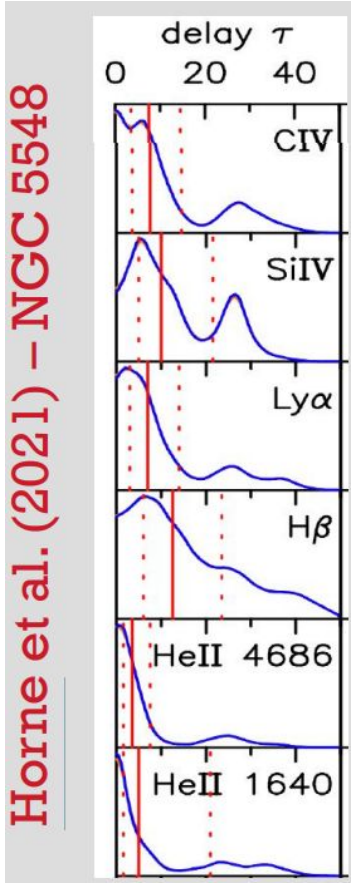

THE UNIFIED MODEL: Stratification and virialization

- **The line width scale with the time delay as $v \sim \tau^{-0.5}$, as expected for a virialized gas dominated by the gravitational potential of the central source:**

  $\langle K \rangle = -1/2 \langle U \rangle$

  $1/2mv^2 = ½\ GMm/R$

  $v \propto 1/R^{½} \propto 1/(c\tau)^{½} \propto 1/(\tau)^{½}$

- **Since the gas appear to be virialized, we can estimate BH masses using virial theorem**

$$M_{\rm BH} = \frac{f c \tau \Delta V^2}{G}$$

Where *f* is a factor that includes (unknown) BLR geometry and inclination.

Masses measured this way appear accurate to within a factor of ~ 3 when Hβ is used.

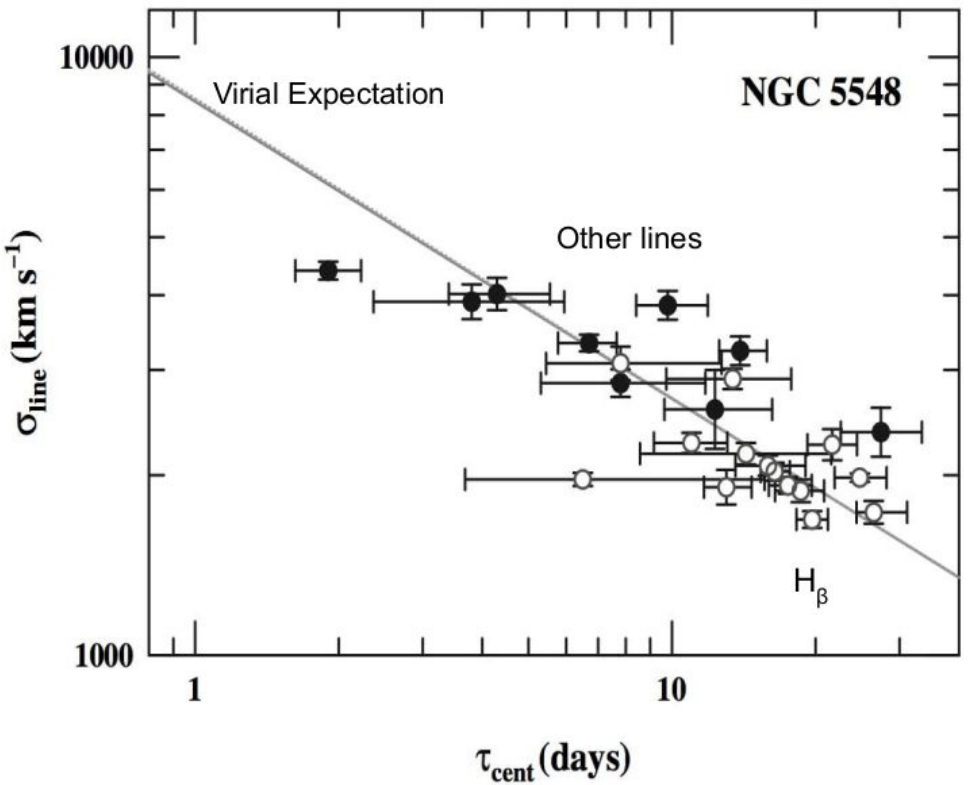

THE UNIFIED MODEL: Stratification and virialization

- **It is possible to combine the R_{BLR}-L relation with the virial theorem to estimate single-epoch masses, e.g.:**

$$\frac{M_{\rm BH}}{10^6\ M_\odot} = 4.35 \left[\frac{\nu L_\nu(5100\ \text{Å})}{10^{44}\ \text{ergs s}^{-1}}\right]^{0.7} \left[\frac{\text{FWHM(H}\beta)}{10^3\ \text{km s}^{-1}}\right]^2$$

- **These allow quick estimates for large AGN samples, but their accuracy is no better than a factor of several. The main challenge is characterizing the line widths, where caution is needed**
- **Statistical use of such masses in large samples is probably OK, but individual mass estimates may be unreliable**

Peterson et al. (2004)

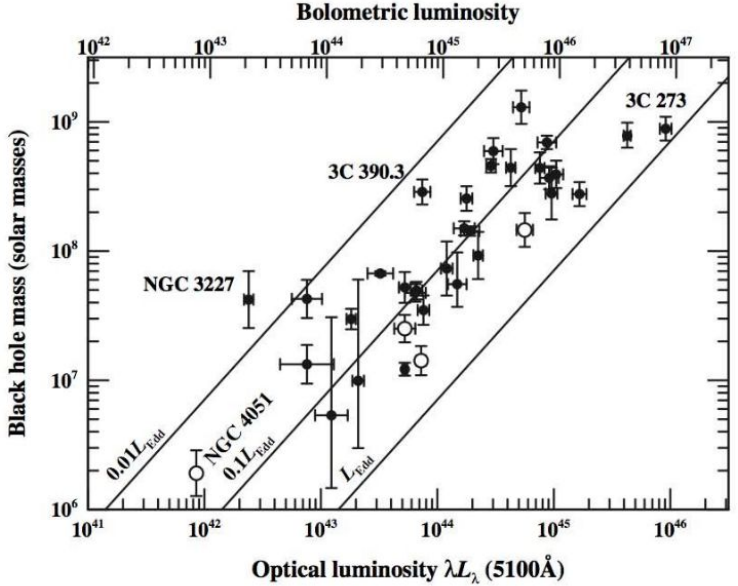

Fig. 9. The mass–luminosity relationship for reverberation-mapped AGNs. The luminosity scale on the lower x-axis is $\log \lambda L_\lambda$ in units of ergs s^{-1}. The upper x-axis shows the bolometric luminosity assuming that $L_{\rm bol} \approx 9\lambda L_\lambda(5100\,\text{Å})$. The *diagonal lines* show the Eddington limit $L_{\rm Edd}$, $0.1L_{\rm Edd}$, and $0.01L_{\rm Edd}$. The *open circles* represent NLS1s. From [25]

THE UNIFIED MODEL: BLR

What is the nature of the BLR?

- **Increasingly evidence that the BLR itself has a composite nature:**
  - **Moderate-ionization and high-optical-depth region**
    - **Largely responsible for the Balmer-line emission and Mg II**
    - **Accretion disk itself?**
    - **A disk with a large line-emitting region can make single-peaked profiles consistent with most objects**
  - **High-ionization and moderate-optical-depth region**
    - **Largely responsible for the high-ionization lines**
    - **Accretion-disk wind?**
    - **Helps explain blueshifts of high-ionization lines and blueward line asymmetries**

- **Line emission may arise in gas lifted from disk by radiation pressure on dust and/or magnetic fields. Any dust is largely destroyed once exposed to the ionizing radiation, allowing efficient line production.**
- **Likely substantial object-to-object variations with other components often present too.**

THE UNIFIED MODEL: BAL & Outflowing winds

Outflowing winds:

- **Blueshifted UV Broad Absorption Lines (BAL) in Quasars are interpreted in terms of outflowing winds**
- **Seen in 10-15 % of sources, but thought to be associated to 20-30% of sources (due to selection effects)**
- **Complex and multiple absorption features; Multiple BALs from same transition probe distinct wind components**
- **Defined to be broader than 2000 km/s; narrower line are often defined as mini-BALs**

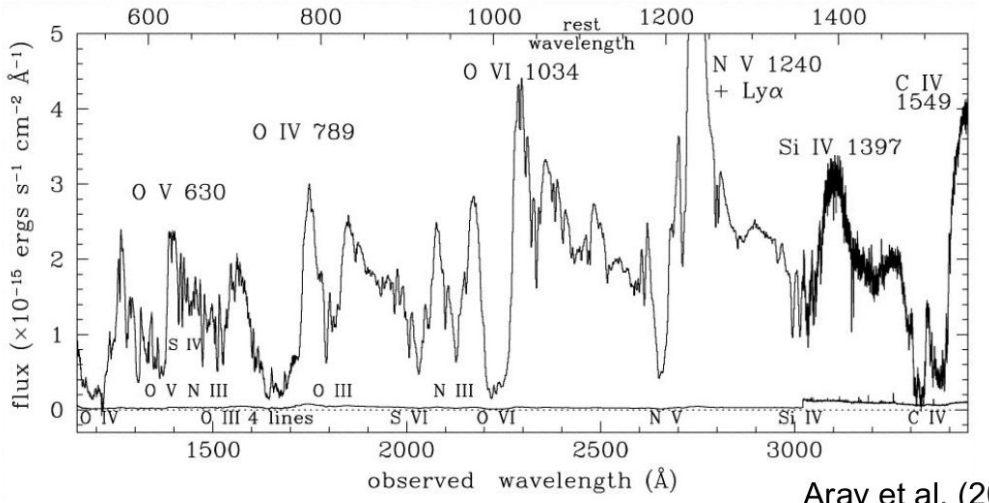

Arav et al. (2001)

THE UNIFIED MODEL: BAL & Outflowing winds

Outflowing winds:

- **Found over a wide AGN Luminosity Range**
- **There is a correlation with luminosity: the larger the luminosity the larger the wind velocity**

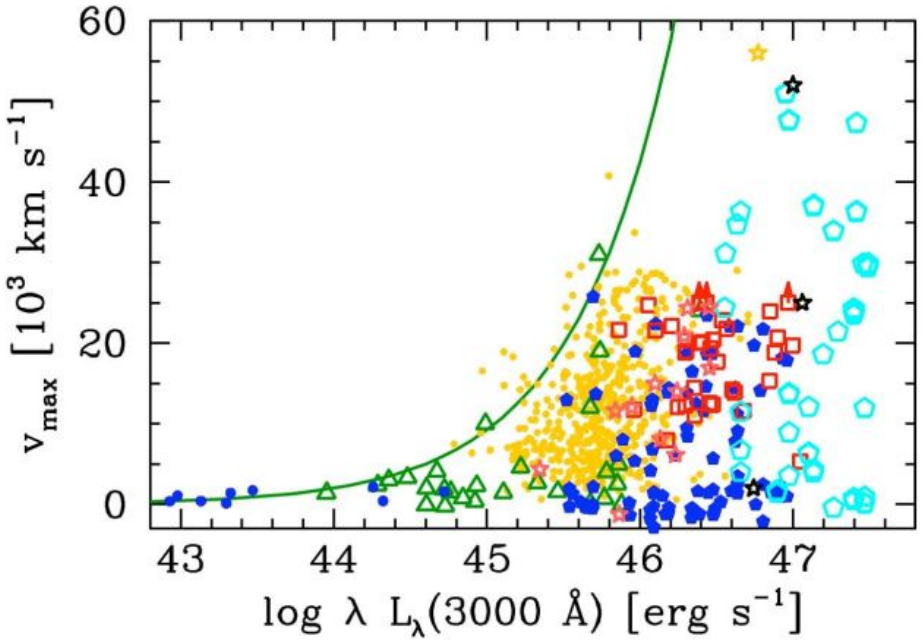

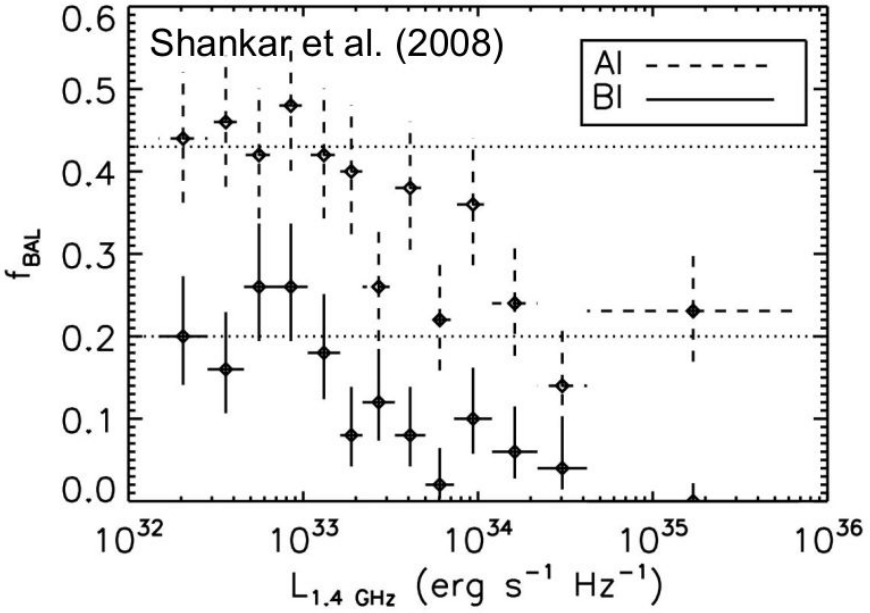

BAL fraction depends upon radio power:

- **BALs generally avoid highly radio-luminous quasars (though not entirely)**
- **Reason for this is still not entirely clear → Wind-jet connection? Orientation effects?**

THE UNIFIED MODEL: BAL & Outflowing winds

Wind model:

- **Most AGNs likely drive winds**
- **Multiple lines from the same transition probe distinct wind components**
- **Wind material exists over a wide range of radii from 0.01 pc to kpc scales. Often outside the BLR.**
- **Wind is driven by radiative pressure on the lines from the Equatorial Accretion-Disk or Torus to Velocities of ~ 100-30000 km/s**

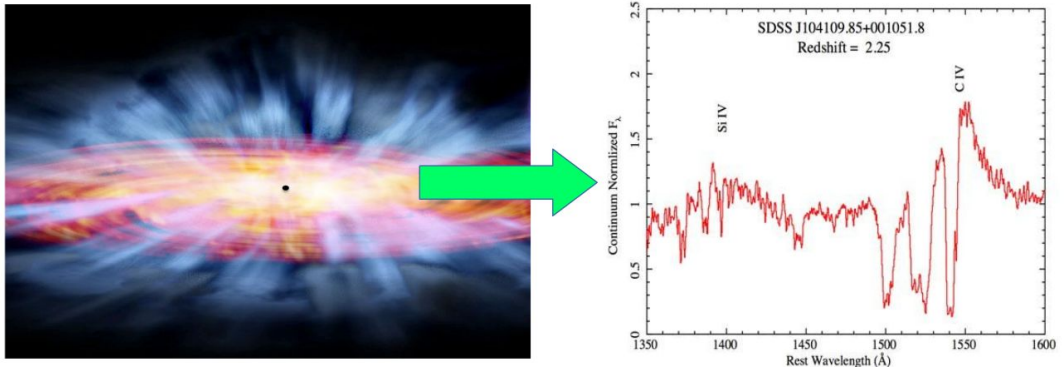

Why we care about AGN winds?

- **Significantly affect observed AGN properties (UV line absorption, high-ionization line emission, reddening, polarization, X-ray absorption)**
- **Substantial part of typical AGN nuclear regions; seen in absorption in ~ 30% of AGNs**
- **Help black-hole accretion to proceed by removing angular momentum from the disk**
- **Can evacuate gas from the host galaxy, likely affecting black-hole growth and galaxy evolution**

THE UNIFIED MODEL: BAL & Outflowing winds

Co-evolution and feedback from Supermassive Black Holes (SMBHs):

- **There is a strong correlation between the properties of the SMBHs and their host galaxies**
  - **The SMBHs and their host galaxy seem to evolve together**
- **Feedback from accreting BH: the central SMBH impart energy, mass, and radiation to the host galaxies**

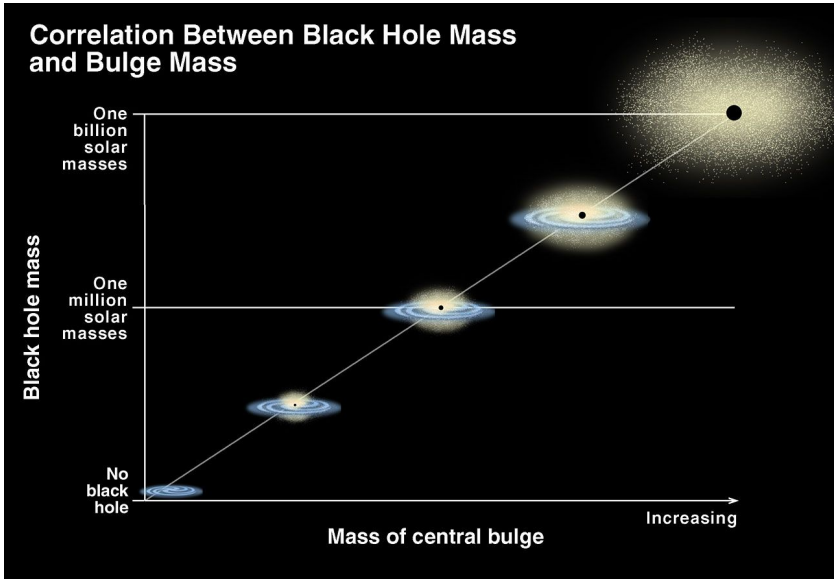

Many BAL quasars likely have $L_K / L_{Edd} > 5\%$ indicating their winds can provide significant galactic feedback.

$$L_k = \frac{1}{2}\dot{M}v^2$$

THE UNIFIED MODEL: BAL & Outflowing winds

Wind feedback into the ISM:

- **Favored in high-density environments.**
- **Radiative losses important.**
- **Momentum injection from AGN drives outflow.**

- **Favored in low-density environments.**
- **Negligible radiative losses**
- **Energy injection from AGN creates hot, over-pressured gas that is the "piston".**

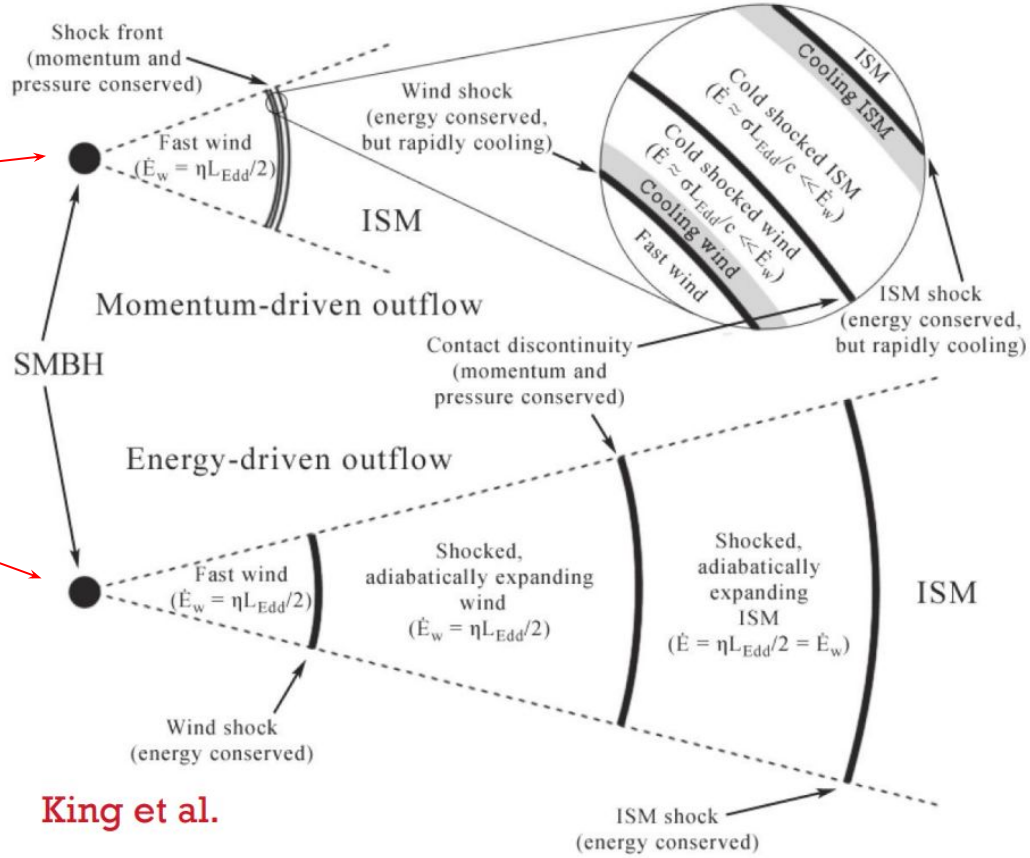

THE UNIFIED MODEL: Narrow Line Region

Imaging the Narrow Line Region (NLR):

- **NLR can be spatially resolved in the optical; has sizes of ~ 100 pc in local Seyferts (and even larger in quasars) → Unlike the BLR, most NLR emission is exterior to the torus**
- **The line emission region is clumpy and complex.**
- **NLR is clearly not spherically symmetric, but rather is roughly axisymmetric.**
- **NLR axis generally coincides with radio axis in cases where extended linear radio emission is detected.**
- **In some sources, we see strong line emission from regions where the radio jet is colliding with the ISM and causing shocks – an additional source of ionization.**

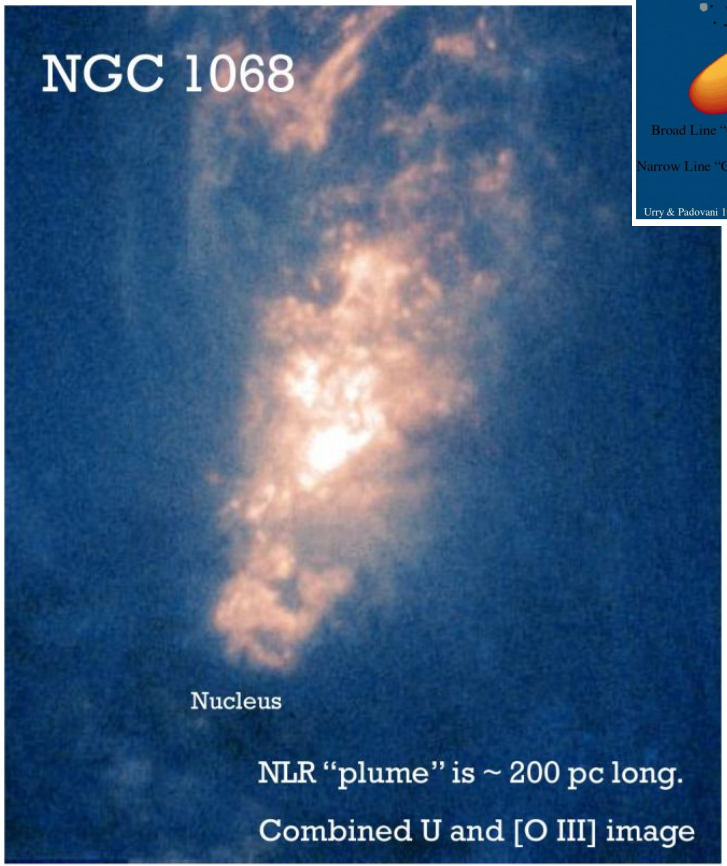

HST - Macchetto et al. (1994)

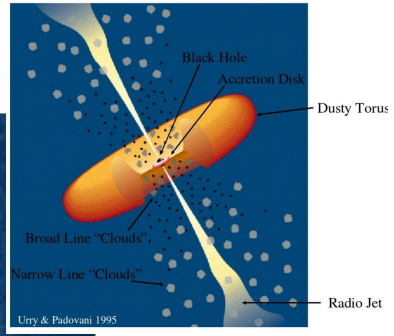

THE UNIFIED MODEL: Narrow Line Region

Narrow Line Region:

- **Narrow components:**
  - **Doppler widths typically less than 900 km/s → FWHM values are 200-900 km/s , with line profiles varying across NLR**
  - **Arise in relatively low-density gas (n_e ~ 10^2 -10^6 cm $^{-3}$) → Presence of forbidden lines**
  - **Do not vary on short timescales**
  - **Wide range of ionization states:**
    - **Low ionization (e.g., [O I] λ6300)**
    - **High ionization (e.g., [O III] λ4959, 5007)**
    - **Sometimes even very highly ionized species (e.g., iron coronal lines)**
- **NLR is the largest spatial scale where ionizing radiation from the AGN dominates.**
- **From line ratios, infer that the NLR is mostly photoionized by the AGN continuum**
- **The wide range of ionization states suggests radial stratification of the NLR**

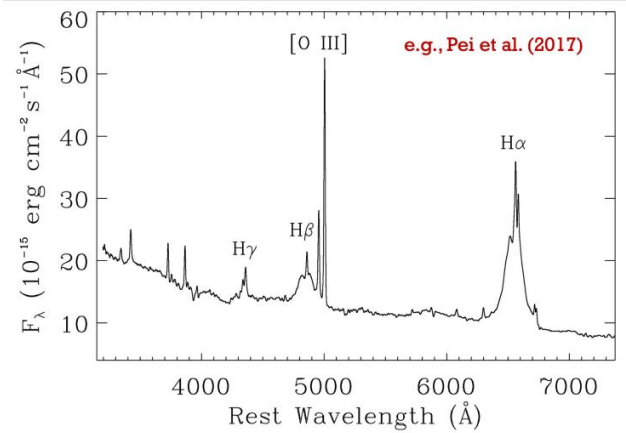

FIG. 1.— Mean spectrum of NGC 5548 from the Asiago dataset, which includes 21 epochs of spectra with spectral resolution of 1.0 Å pixel^{-1} and has a median SNR of 160.

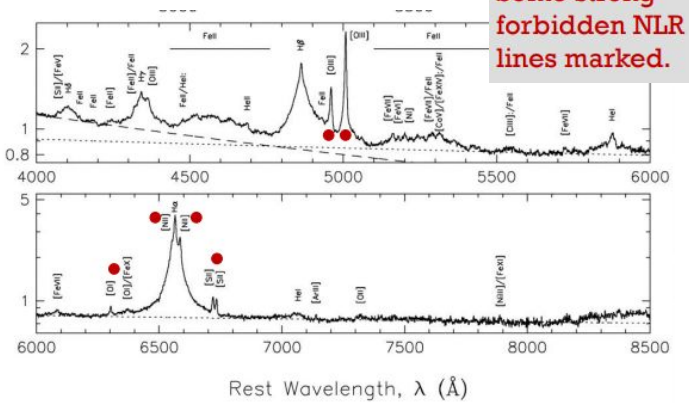

THE UNIFIED MODEL: Narrow Line Region

Narrow Line Region:

- **NLR line equivalent widths drop with increasing continuum luminosity (as for the BLR), and NLR lines are sometimes undetectable in high-luminosity quasars**
  - **Perhaps more luminous AGNs evacuate/destroy ISM gas clouds, leaving less large-scale diffuse gas for NLR emission.**
- **Even at ~ fixed continuum luminosity, there is a wide range of NLR line strength**

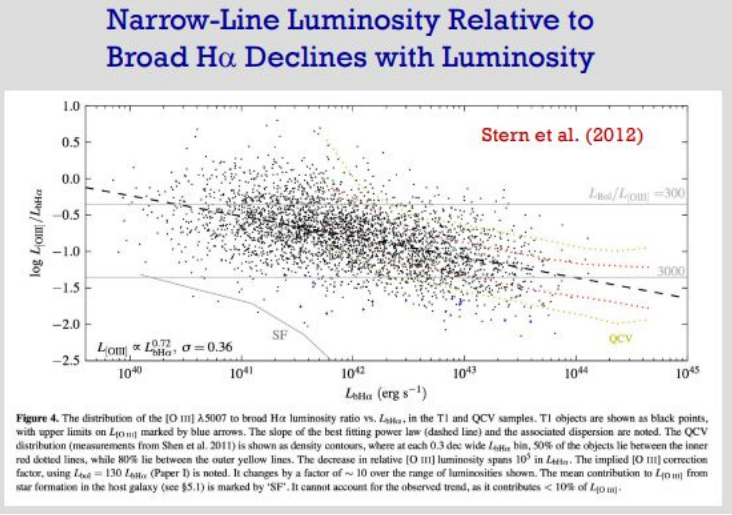

Figure 4. The distribution of the [O III] λ5007 to broad Hα luminosity ratio vs. $L_{H\alpha}$, in the T1 and QCV samples. T1 objects are shown as black points, with upper limits on $L_{[O\,III]}$ marked by blue arrows. The slope of the best fitting power law (dashed line) and the associated dispersion are noted. The QCV distribution (measurements from Shen et al. 2011) is shown as density contours, where at each 0.3 dex wide $L_{bH\alpha}$ bin, 50% of the objects lie between the inner red dotted lines, while 80% lie between the outer yellow lines. The decrease in relative [O III] luminosity spans 10^2 in $L_{bH\alpha}$. The implied [O III] correction factor, using $L_{bH\alpha} = 130\ L_{bH\alpha}$ (Paper I) is noted. It changes by a factor of ~ 10 over the range of luminosities shown. The mean contribution to $L_{[O\,III]}$ from star formation in the host galaxy (see §5.1) is marked by 'SF'. It cannot account for the observed trend, as it contributes < 10% of $L_{[O\,III]}$.

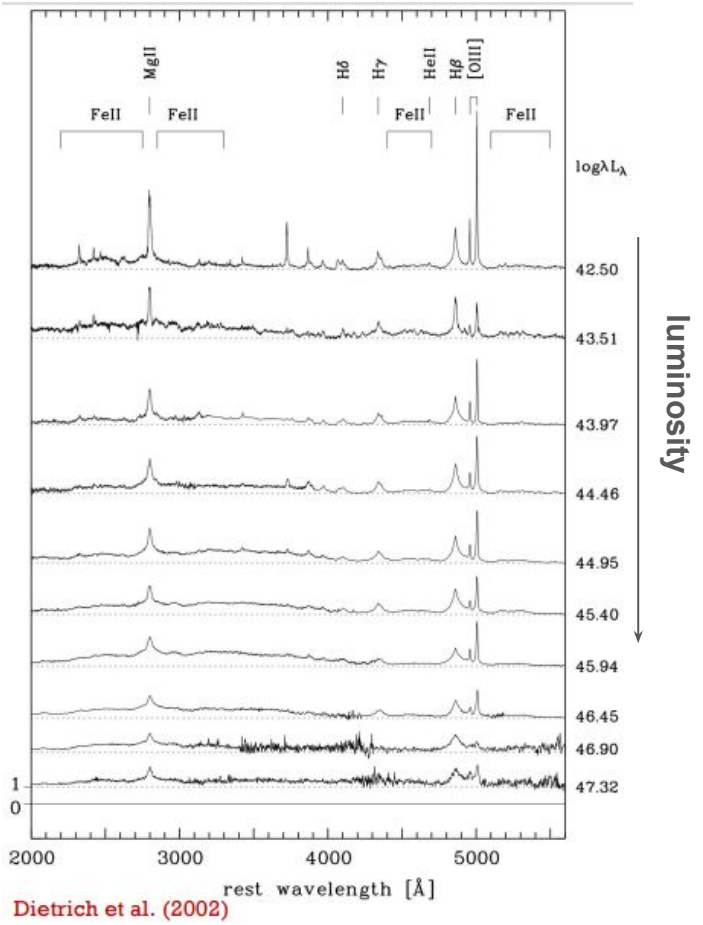

THE UNIFIED MODEL: Narrow Line Region

Importance of NLR:

From the NLR we can map out physical and kinematic properties directly:

- **Line peaks provide useful systemic redshifts for AGNs.**
- **Useful as a bolometer for inferring AGN total power.**
  - **NLR lines can be used to estimate rough bolometric luminosities, even for obscured AGNs.**
  - **Emitted from a region larger than any nuclear obscuration → Vary on longer timescales (decades).**
- **NLR line widths are correlated with host-galaxy bulge luminosity (and bulge gravitational potential)**
- **Anisotropic illumination provides clues about AGN geometry and orientation**
  - **The fairly sharp edges of ionization cones are defined by the collimation of light from the AGN. Collimation could be due to "shadowing" by the torus**

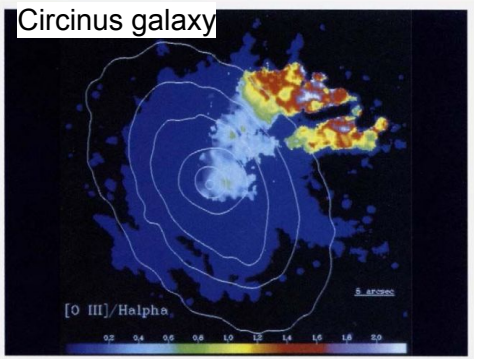

Figure 6: *[OIII]/(Hα+[NII]) showing the ionization structure of the cone. The uniform dark blue region is where Hα+[NII] but not [OIII] was detected at more than 10σ.*

Marconi et al. (1994)

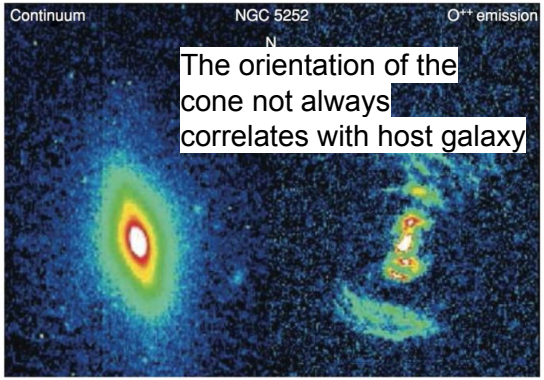

Netzer (2013)

THE UNIFIED MODEL: the torus

Type 1 vs Type 2 AGNs

To first approximation, the optical/UV spectra of AGNs separate into two broad spectral types:

- **Type 1:**
  - **Broad permitted emission lines, specifically the Balmer lines**
  - **Permitted lines clearly broader than forbidden lines**
  - **Moderate EW forbidden lines**
- **Type 2:**
  - **Narrow permitted emission lines, specifically the Balmer lines**
  - **Permitted lines have the same widths as the forbidden lines**
  - **High EW forbidden lines**

These were first defined for Seyfert galaxies, but also apply to quasars.

There are additional complications to this simple scheme (e.g., intermediate type classifications, narrow-line Type 1 AGNs)

Type I example

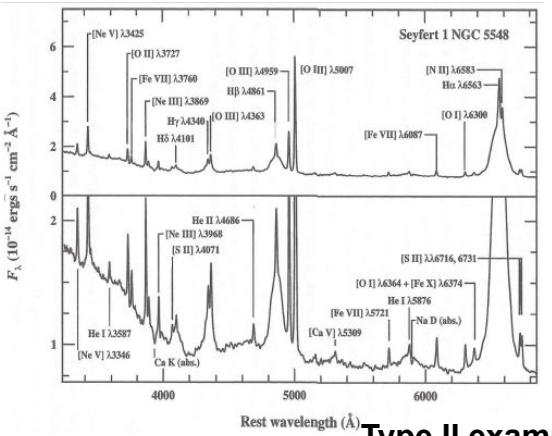

Type II example

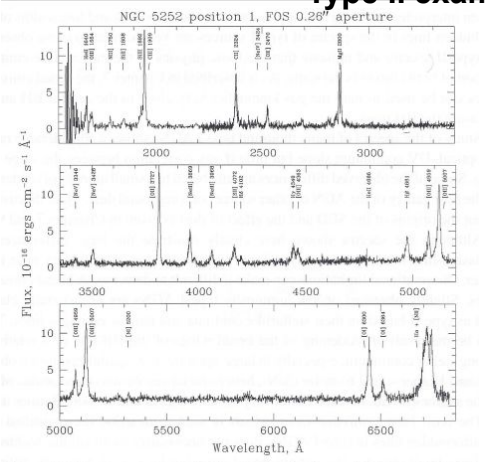

Figure 1.3. The spectrum of the low-luminosity, low-redshift type-II AGN NGC 5252 (courtesy of Zlatan Tsvetanov).

THE UNIFIED MODEL: the Torus

The Type 1 vs. Type 2 optical spectral differences have come to be understood as due to orientation-dependent central obscuration by a so-called "torus":

- **The torus is presumed to be a thick axisymmetric structure of large height (H/R) so that, at least at low luminosities, the majority of AGNs are obscured by it.**
- **It is made of a combination of dusty atomic and molecular gas**
  - **The dust causes large extinction in the optical/UV and sometimes even in the NIR**
- **The torus lies between the BLR and the NLR**
- **Keplerian velocities at the torus distance are ~ 1000 km/s**
- **Density of torus "clumps" are ~ 10^{5} -10^{7} cm^{-3}**
- **The estimated mass of the torus is only a small fraction of the SMBH mass.**

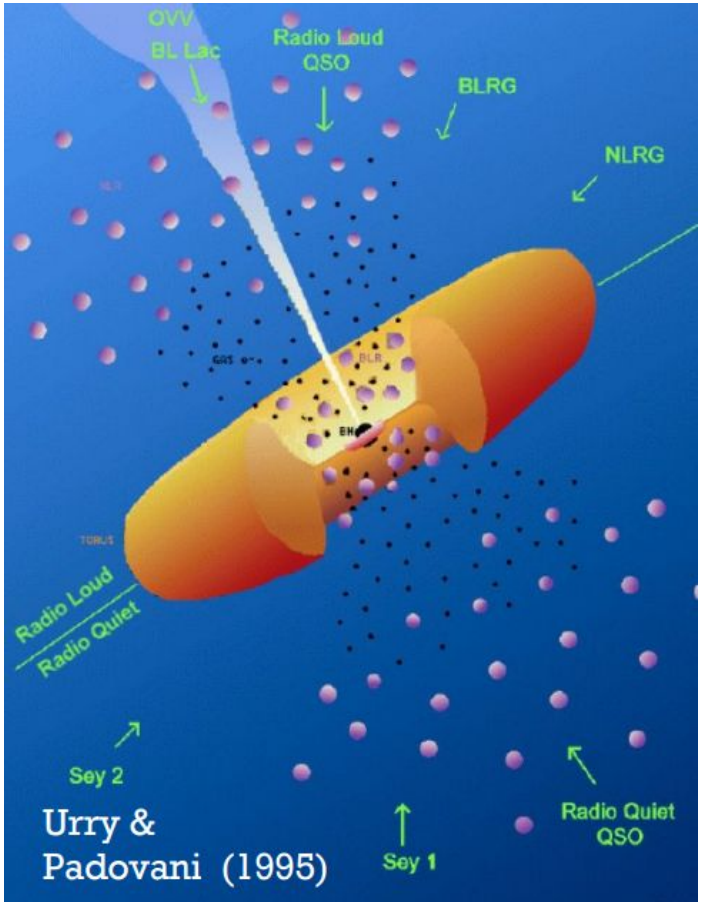

THE UNIFIED MODEL: the Torus

Example of hidden BLR in Type 2 AGN revealed using spectropolarimetry

The scattering polarizes the relevant radiation, with the polarization position angle perpendicular to the system axis (from jet/ionization cone)

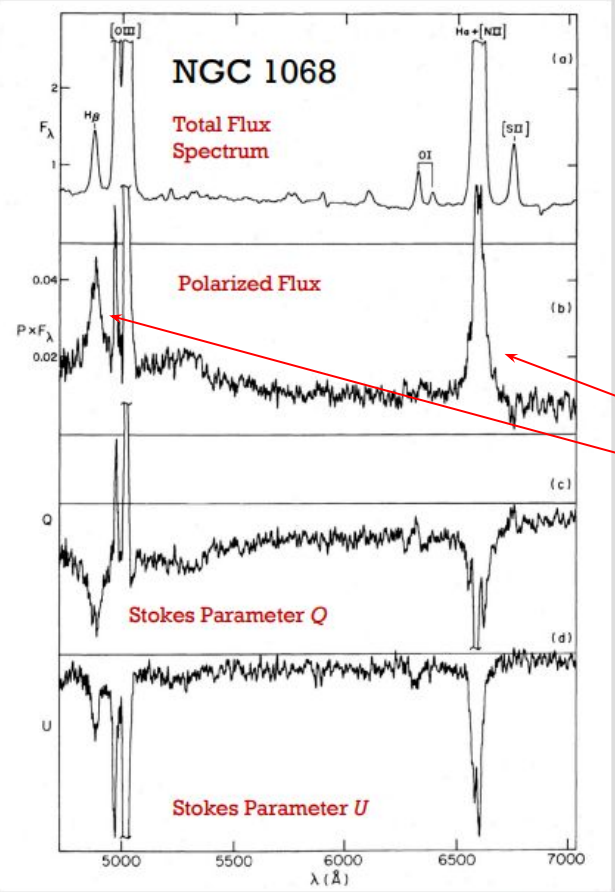

Antonucci & Miller (1985); also see Antonucci (1984) on 3C234

b) Structure in the Polarization Spectrum: The Seyfert 1 inside NGC 1068

There is a great deal of structure in the polarization spectrum. As explained in Paper I, much of it is due to dilution of a featureless continuum by unpolarized starlight. We see many stellar absorption lines "in emission" in the polarization spectrum, because there is less starlight reducing P at those wavelengths. Similarly we can see the stellar continuum breaks in $P(\lambda)$. As we noted in Paper I, $P(\lambda)$ really looks like a galaxy spectrum plotted upside down.

There are some polarization features that cannot be explained by dilution. We noted in Paper I that there is a polarization excess redward of each narrow Balmer line, and in studying our data more carefully, we also see small excesses in *P blueward* of Hα and Hβ. There is also excess polarization in the 4500–4600 Å region. McLean *et al.* (1983) find similar structure in $P(\lambda)$. Interpretation of these features appears to provide the key to the NGC 1068 polarization, and it is the most important part of this paper.

Plots of polarized flux, $P(\lambda) \times F(\lambda)$, eliminate the effects of unpolarized starlight, and suppress low-polarization line emission. Figures 1 and 2 show the polarized flux, and the appearance of these figures is surprising. They look like the spectra of a Seyfert Type 1 object! Broad symmetric Balmer lines and Fe II emission are clearly seen. The Balmer line full widths at zero internsity are ~7500 km s^{-1}. The presence of Fe II is crucial in establishing that this broad emission comes from clouds of very high optical depth. We can draw several rather

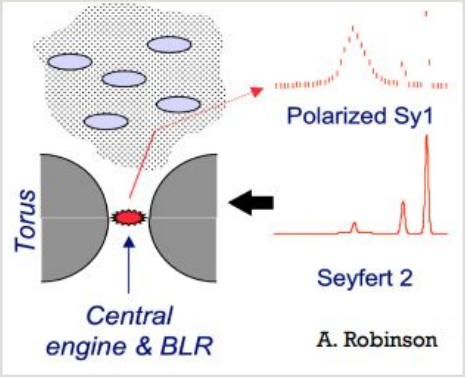

THE UNIFIED MODEL: the Torus

Burtscher et al. 2016

Size of the Torus:

- **It can be directly measured using:**
  - **Dust reverberation mapping between the V-band and K-band light curves.**
  - **Interferometry in the NIR and MIR mapping the hot inner wall and the cool dust.**
  - **The torus spans a wide range of radii and temperatures, so methods at different wavelengths will deduce different sizes**
- **The size of the inner boundary appears to scale as $L^{0.5}$ (consistent with constant ionization parameter)**
- **The inner edge of the torus is at about 3 times the BLR radius for Hβ as determined from reverberation mapping**

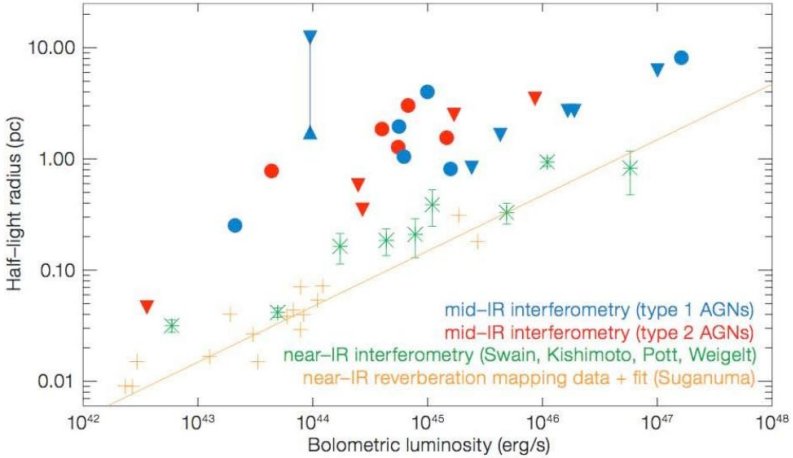

Figure 5. Size–luminosity relation for AGNs probing different regions of the torus: blue/ red points are MIDI measurements from the MIDI AGN Large Programme + archive for type 1/type 2 sources (statistical errors are smaller than symbol sizes); green crosses are NIR interferometry with both the Keck-Interferometer and AMBER/VLTI; orange pluses are from NIR dust reverberation mapping. Filled triangles show limits. Taking both the limits and the determined half-light radii into account shows that the mid-infrared size is less strictly correlated with luminosity than the innermost radius of dust that is seen in the NIR.

THE UNIFIED MODEL: the Torus

Molecular Torus Imaging

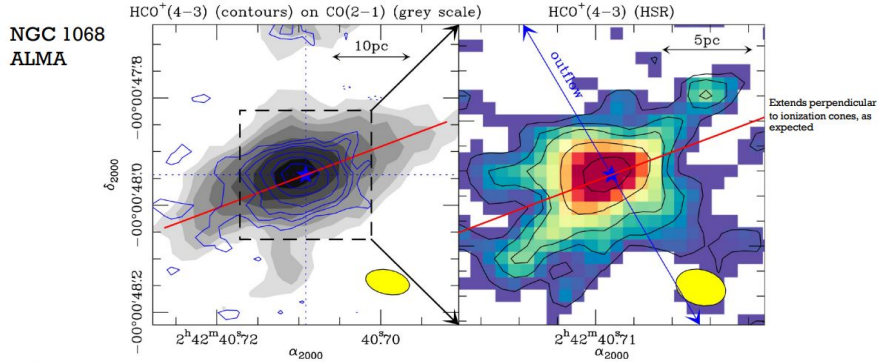

Fig. 25. Overlay of the HCO$^+$(4–3) (blue) contours on the CO(2–1) grayscale image of the molecular torus of NGC 1068 derived from the MSR data set (*left panel*). We show a zoomed view of the inner $r = 0.''12 \simeq 8$ pc of the molecular torus obtained from the HSR data set in the *right panel*. Contours and intensity scales are the same as in Figs. 11 and 12. The continuous (blue) line shows the axis of the large-scale ionized outflow. The (red) line shows the orientation of the kinematic major axis of the CO(2–1) torus derived in Sect. 7.1 by ^{3D}Barolo (PA = 291° = 180° + 111°). The (yellow) filled ellipses show the ALMA beam sizes.

Thermal Torus Imaging for NGC 1068

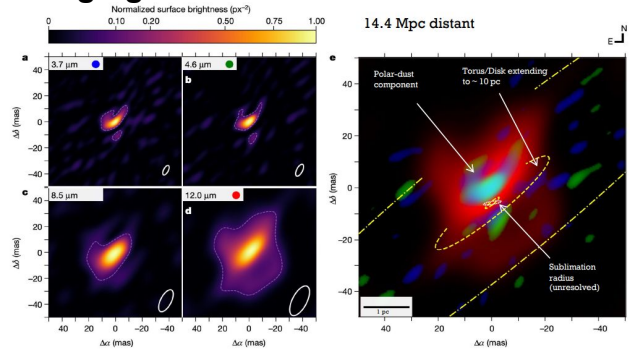

Fig. 1 | IRBis reconstructed images of NGC 1068. a–d. Images are derived from L, M and N bands at median wavelengths of 3.7 μm (**a**), 4.6 μm (**b**), 8.5 μm (**c**) and 12 μm (**d**). The dashed white contours indicate the 3σ noise level and the white ellipses indicate the resolution. **e.** Red–green–blue composite colour image of the 3.7 μm (blue), 4.6 μm (green) and 12 μm (red) images. The ellipses in the composite image illustrate the possible midplane of the inhomogeneous obscuring layer discussed in section 'Spatial distribution of the dust'. The innermost small ellipses indicate two possible positions of the masked sublimation limit around the position of the supermassive black hole, and the outermost dot-dashed ellipse shows the maximum measured disk extent (10 pc). Scale bar, 1 pc. $\Delta\alpha$ and $\Delta\delta$ are the position offsets from the brightest feature, measured in true mas, in the right ascension and declination directions, respectively.

MATISSE/VLTI

Large-Scale Polar Dust Emission

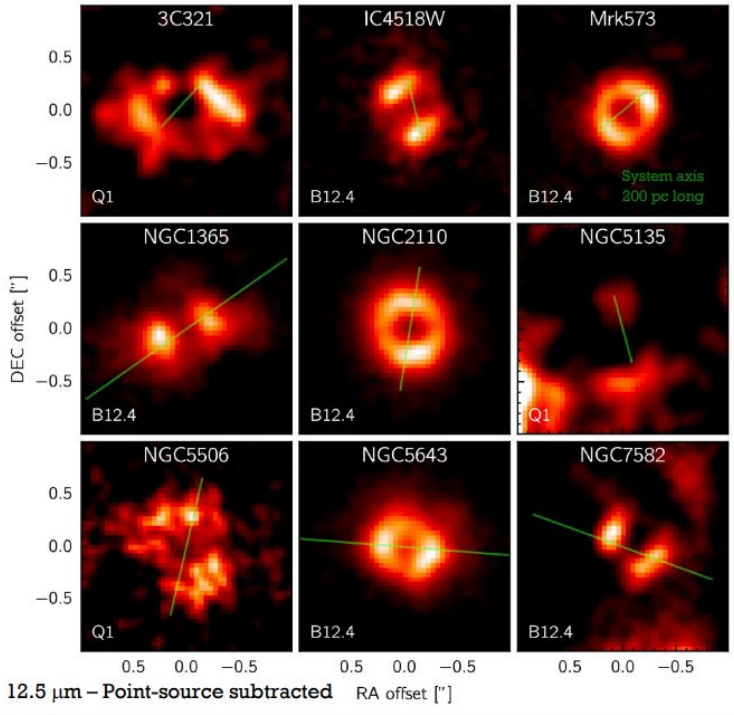

THE UNIFIED MODEL: the Torus

- **Overall, the "torus" appears to be a multi-component structure (clumpy disk + clumpy wind?) with complex dynamics.**
- **Spans sub-pc to tens of pc scales.**
  Structure depends on AGN properties
- **Large ~ random source-to-source variations**

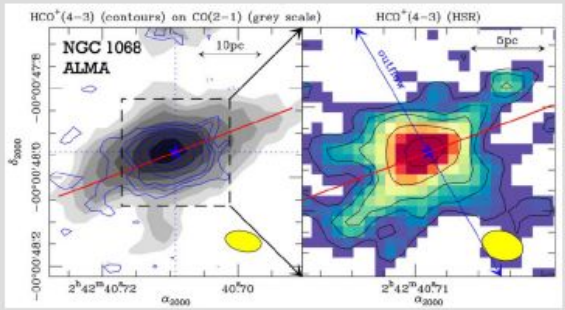

García-Burillo et al. (2019)

+

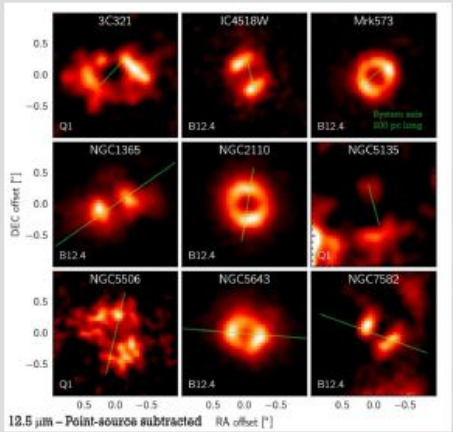

Asmus (2019)

≈

Clumpy disk + Clumpy Wind

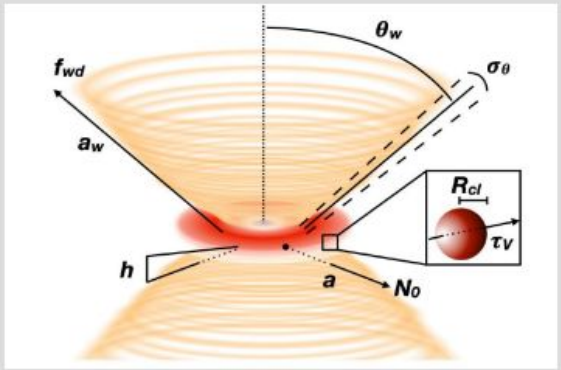

e.g., Hönig & Kishimoto (2017);
Alonso-Herrero et al. (2021)

?

THE UNIFIED MODEL: Jets

- ~10% of optically luminous AGNs host a relativistic jets of particles
- The jets produce strong radio emission, primarily via synchrotron
  - Such AGNs are termed “radio loud”
- Jets often appear relativistic based on beaming, apparent superluminal motions on sub-pc scales, and variability
  - Thus, the apparent properties of a jet depend strongly upon orientation
- At least in some cases, jets are launched on very small scales (making much of the “core” radio emission)
- They can be collimated over a huge range of scales
- Jets are often seen in the X-ray and also the optical

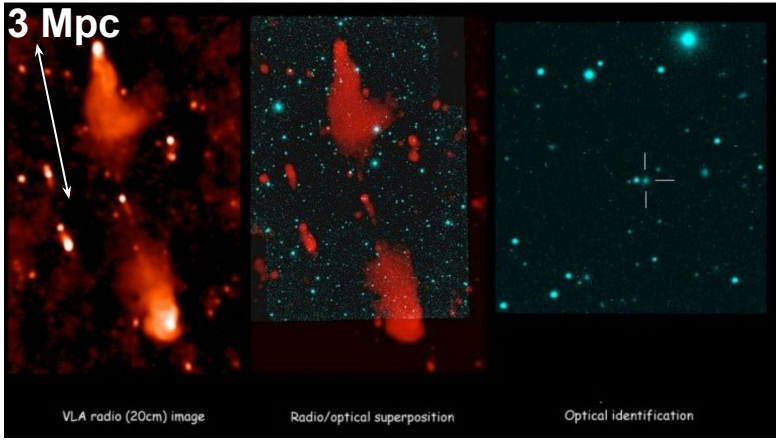

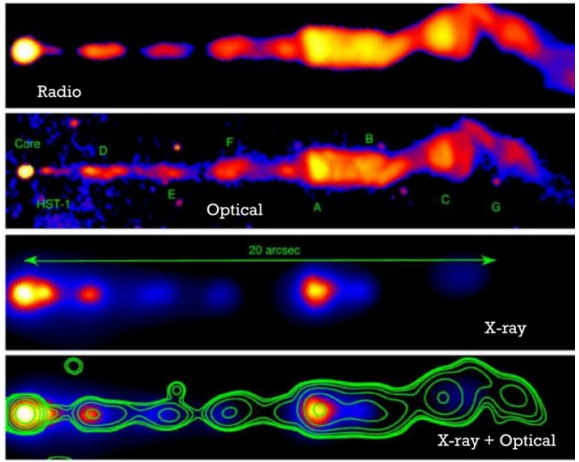

THE UNIFIED MODEL: Jets

Flat vs. Steep Spectrum Radio Sources

- Often observe radio power-law spectra: $L_\nu \sim \nu^{-\alpha}$
- Radio-loud AGNs with dominant radio cores usually show “flat” radio spectra with $\alpha < 0.5$
- Radio-loud AGNs with dominant lobes usually show “steep” radio spectra with $\alpha > 0.5$
- Much of the difference in measured value of α is due to inclination of radio jet to our line-of-sight

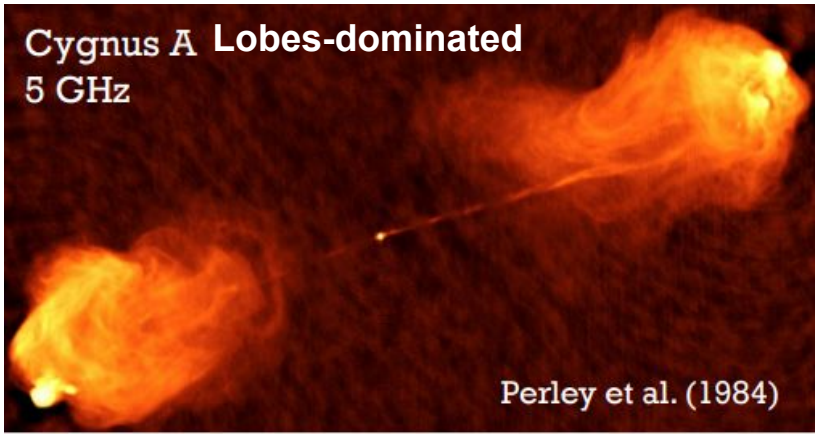

Core-dominated

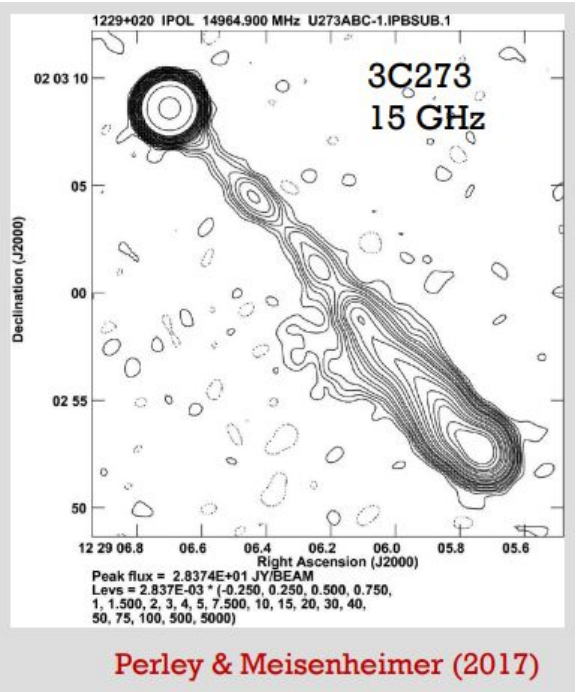

THE UNIFIED MODEL: Jets

AGN feedback in clusters: jets can do substantial work against the hot gas in galaxy clusters

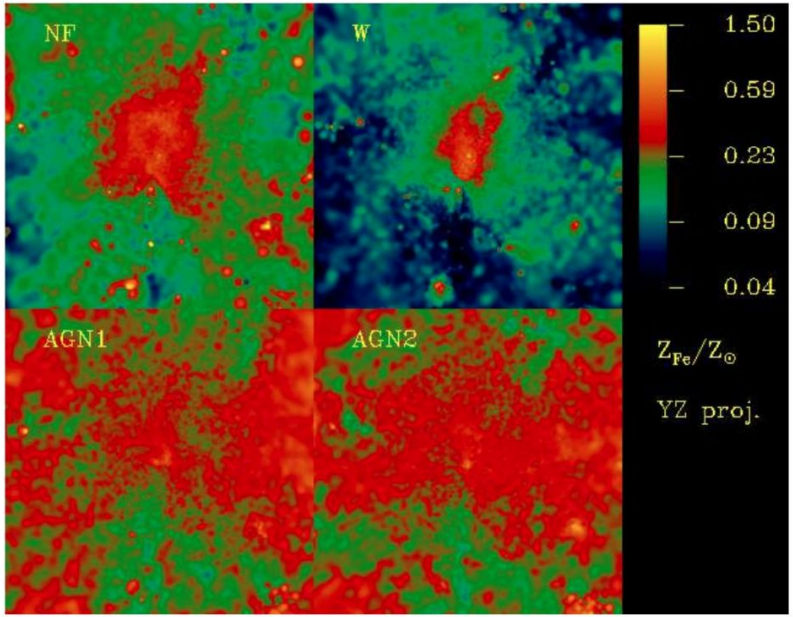

Figure 7. Maps of emission weighted Fe abundance in the g51 cluster for the runs without feedback (NF, top left), with winds (W, top right) and with AGNs (AGN1 and AGN2, bottom left and bottom right, respectively). Each map has a side of $2R_{vir}$. Abundance values are expressed in units of the solar value, as reported by Grevesse & Sauval (1998), with color coding specified in the right bar.

Fabjan+10

Buoyant cavities in the ICM

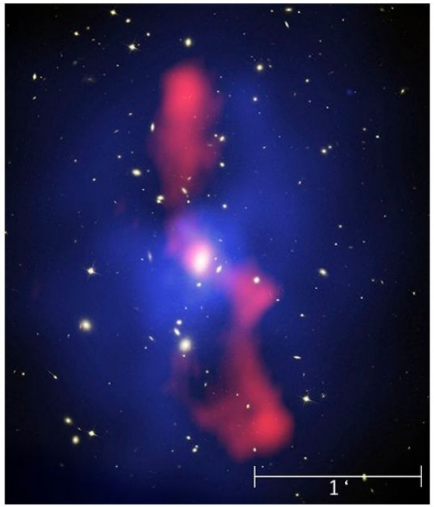

McNamara et al. (2005)

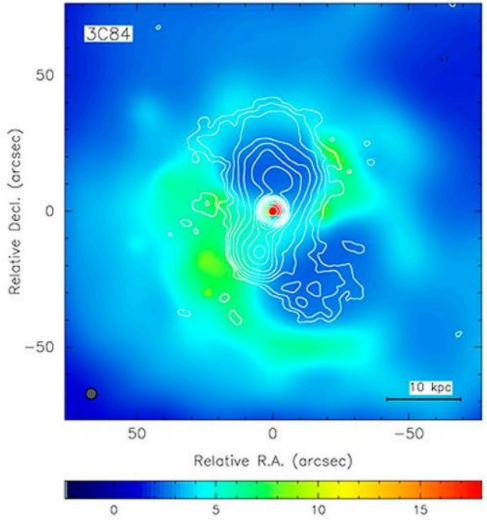

Fabian et al. (2003)

THE UNIFIED MODEL: Jets

How are jets made?

- **An accreting, spinning SMBH model has promising and observationally supported "ingredients" for making jets:**
  - **Relativistically deep potential well**
  - **Preferred axis that is stable – "gyroscope"**
  - **Large energy reservoirs**
  - **Magnetic fields in orbiting and jet plasma**
- **Generally, models invoke MHD processes to divert some of the inflowing plasma outward and then keep it collimated.**
- **But exactly how to combine the "ingredients" remains poorly understood**
- **What sets if a strong jet will be launched?**
  - **SMBH spin?**
  - **Magnetic field properties?**
  - **Environment?**

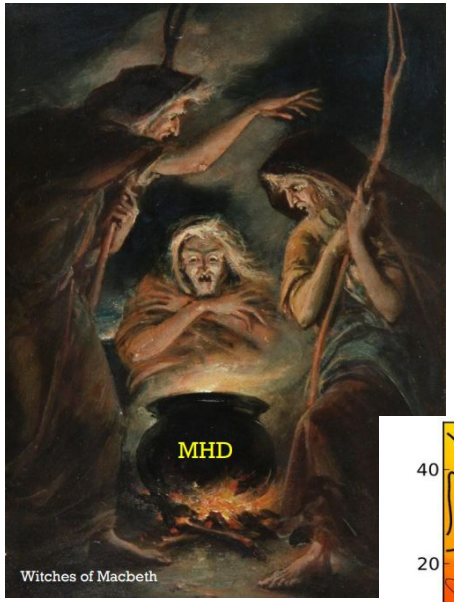

Simulations of accretion flows on spinning SMBH. See Davis & Tchekhovskoy et al. (2020), Blandford et al. (2019), Blandford & Globus (2022) and references therein to learn more.